# NATIONAL ADVISORY COMMITTEE FOR AERONAUTICS

## TECHNICAL NOTE 4191

ANALYSIS OF HORIZONTAL-TAIL LOADS IN PITCHING MANEUVERS

ON A FLEXIBLE SWEPT-WING JET BOMBER

By William S. Aiken, Jr.

Langley Aeronautical Laboratory
Langley Field, Va.

NACA

Washington

December 1957

NATIONAL ADVISORY COMMITTEE FOR AERONAUTICS

TECHNICAL NOTE 4191

ANALYSIS OF HORIZONTAL-TAIL LOADS IN PITCHING MANEUVERS

ON A FLEXIBLE SWEPT-WING JET BOMBER

By William S. Aiken, Jr.

## SUMMARY

Horizontal-tail loads measured by means of strain gages in pitching maneuvers are analyzed to determine wing-fuselage aerodynamic-center position, zero-lift pitching-moment coefficient, airplane pitching moment of inertia, and radius of gyration. A similar analysis is made of the time-history data for the elevator angles and the results were found to agree with those from the tail-load analysis. The flight-determined values of aerodynamic-center position for rigid conditions and the zero-lift pitching-moment coefficients were in some disagreement with the wind-tunnel data over the Mach number range of the tests (0.42 to 0.81). The pitching moment of inertia determined from the flight data for rigid-wing conditions agreed with calculations based on ground tests. The effective pitching moment of inertia computed from theoretical consideration for flexible flight conditions was in disagreement with flight data. Details of the analysis procedures and least-squares methods used are given.

## INTRODUCTION

The calculation of airplane design tail loads and stability characteristics requires reliable estimates of the wing-fuselage pitching-moment characteristics. The use of highly swept flexible wings combined with other flexible airplane components introduces additional factors which must be considered in tail-load design analysis procedures. Investigations by the National Advisory Committee for Aeronautics of a large flexible swept-wing jet bomber which included measurements of horizontal-tail loads permitted the analysis of data from which comparisons could be made between wind-tunnel measurements of wing-fuselage aerodynamic-center positions and zero-lift pitching-moment coefficients and values of these parameters as derived from flight data.

The analysis of flight data in the present report is, to a large extent, based on analyses and information contained in references 1

and 2 for wing deflections, reference 3 for horizontal-tail parameters, reference 4 for airplane lift-curve slopes and angles of zero lift, and reference 5 for wing centers of pressure. The methods used to analyze the flight data and to convert measured pitching-moment parameters to equivalent rigid conditions for comparison with wind-tunnel data are described in detail. Comparisons are given between flight and wind-tunnel results for aerodynamic-center position and zero-lift pitching-moment coefficients and between flight and calculated values of moments of inertia and radii of gyration for both flexible and rigid conditions. Although no direct comparisons are made with present tail-load design computation methods, the theoretical methods which were used in the flight-data analysis contain the essential elements of design procedures for flexible aircraft and, thus, provide an indirect check on their adequacy.

## SYMBOLS

$A, B, C, D$      coefficients of equations (A7) and (B1) used to obtain airplane pitching-moment parameters

$A_{corr}$      the $A$ coefficient of equation (B1) corrected for zero shift

$C_{L_{\alpha_t}}$      horizontal-tail lift-curve slope per degree

$\left(C_{L_{\alpha_t}}\right)_f$      horizontal-tail lift-curve slope per degree for flexible fuselage conditions defined by the expression

$$\frac{C_{L_{\alpha_t}}}{1 - \dfrac{di_t}{dL_t} C_{L_{\alpha_t}} qS_t}$$

$C_{L_\delta}$      horizontal-tail lift-curve slope per degree with root elevator angle

$C_{m_\delta}$      tail pitching-moment coefficient due to elevator deflection

$C_{m_0}$      zero-lift wing-fuselage pitching-moment coefficient

$C_{m_{0_M}}$      zero-lift wing-fuselage pitching-moment coefficient computed directly from measured zero-lift tail load

$C_{M_{0_I}}$      corrected zero-lift wing-fuselage pitching-moment coefficient using analysis method I

$C_{m_{O_{II}}}$   zero-lift wing-fuselage pitching-moment coefficient using analysis method II

$C_{N_{A_C}}$   airplane normal-force coefficient corrected for pitching-acceleration tail load

$I_y$   airplane pitching moment of inertia, slug-ft$^2$

$I_{y_f}$   effective airplane pitching moment of inertia defined by equation (A10), slug-ft$^2$

$L_t$   aerodynamic tail load, lb

$L_{t_T}$   aerodynamic tail load plus component of tail aerodynamic pitching moment defined by equation (A6), lb

$L_w$   aerodynamic wing load, lb

$L_{w_{\ddot\theta}}$   aerodynamic wing load per unit pitching acceleration,
$$\frac{lb}{radian/sec^2}$$

$L_{\dot\theta}$   aerodynamic wing load due to pitching velocity (eq. (A3)), lb

$L_{\ddot\theta}$   aerodynamic wing load due to pitching acceleration (eq. (A2)), lb

$M$   Mach number

$M_{ac}$   pitching moment about wing-fuselage aerodynamic center

$N$   number of equations in least-squares solutions

$S$   wing area, sq ft

$S_t$   horizontal-tail area, sq ft

$T_t$   tail aerodynamic torque, in-lb

$V$   true airspeed

$W$   airplane weight, lb

$W_t$   horizontal-tail weight, lb

$X_{cg}$      location of airplane center of gravity, percent $\bar{c}$

$(X_{ac})_r$      location of rigid-wing—fuselage additional-load aerodynamic center, percent $\bar{c}$

$(X_{ac})_{flex}$      location of flexible-wing—fuselage additional-load aerodynamic center, percent $\bar{c}$

$X_{\ddot{\theta}}$      location of center of pressure of aerodynamic wing load due to pitching acceleration, percent $\bar{c}$

$Z'$      zero shift in measured aerodynamic tail loads (from ref. 3), lb

$Z_T$      zero shift in measured aerodynamic tail torque, in-lb

$a_F$      faired tail-on airplane lift-curve slope per degree (from ref. 4)

$\bar{c}$      wing mean aerodynamic chord, in.

$\bar{c}_t$      tail mean aerodynamic chord, in.

$d$      distance from wing-fuselage aerodynamic center to airplane center of gravity, positive with center of gravity forward of the aerodynamic center, in.

$d_{\ddot{\theta}}$      center of pressure of wing load due to pitching acceleration, in.

$d_{\dot{\theta}}$      center of pressure of wing load due to pitching velocity, in.

$g$      acceleration of gravity, ft/sec$^2$

$i_t$      tail incidence, deg

$i_w$      wing incidence, deg

$k_y$      airplane radius of gyration in pitch, ft

$k_{y_f}$      effective airplane radius of gyration in pitch, ft

$l_t$      horizontal-tail length, distance from airplane center of gravity to quarter-chord of horizontal-tail mean aerodynamic chord, in.

$m_R$            rigid-wing—fuselage lift-curve slope per degree

$n$            normal load factor at airplane center of gravity

$n_t$            normal load factor at horizontal tail

$q$            dynamic pressure, lb/sq ft

$w$            weighting factors

$x_t$            distance from wing-fuselage aerodynamic center to quarter-chord of horizontal-tail mean aerodynamic chord, in.

$\Delta X_{ac}$            difference between rigid- and flexible-wing—fuselage aerodynamic-center positions, defined by equation (6), percent $\bar{c}$

$\Delta k_{y_f}^2$            difference between theoretical and measured $k_{y_f}^2$ values, ft$^2$

$\alpha_t$            tail angle of attack, deg

$\alpha_w$            wing angle of attack, deg

$\alpha_{0_{adj}}$            wing angle of zero lift (from ref. 4), deg

$\delta$            root elevator angle, positive down, deg

$\delta_0$            root elevator angle at zero load factor, deg

$\epsilon$            errors in fit or measurements; subscripts to $\epsilon$ denote error associated with quantity indicated

$\epsilon_1$            error in calculated $k_{y_f}^2$

$\epsilon_2$            error in measured $k_{y_f}^2$

$\dot{\theta}$            pitching velocity, radian/sec

$\ddot{\theta}$            measured pitching acceleration corrected for instrument response characteristics, radian/sec$^2$

$\sum$            indicates summation

$d\epsilon/d\alpha$          effective downwash factor

Matrix notation:

$\{\ \}$          column matrix

$\|\ \|$          rectangular matrix

$\|\ \|^T$          transpose of rectangular matrix

$[\ ]^{-1}$          inverse of square matrix

    Bars over symbols indicate average values.


APPARATUS AND TESTS


Airplane

    The airplane used for this investigation was a six-engine, jet-propelled medium bomber. A photograph of the test airplane is shown as figure 1, and the airplane and horizontal-tail characteristics and dimensions are given in table I.


Instrumentation

    The data used for analysis in the present paper were obtained from standard NACA recording instruments and from strain gages mounted on the right and left sides of the horizontal tail.

    Normal accelerations were measured by two air-damped accelerometers, one near the center of gravity and one at the horizontal tail. Angular accelerations in pitch were measured by a rate-gyro type, electrically differentiating, magnetically damped turnmeter. Airspeed and altitude measurements were made with an NACA pitot-static head mounted on a boom approximately 1 maximum fuselage diameter ahead of the original nose.

    Electrical wire-resistance strain gages (Type A-6) with low temperature correction factors were used to measure the root shears, bending moments, and torques at stations on the right and left sides of the tail. The gages were installed as four-active-arm bridges on the web and flanges of the main spars (50 percent chord) and on the upper and lower skin surfaces near the leading edges of the horizontal tail.

The strain-gage bridge installation was calibrated according to the method detailed in reference 6. The bridges were then combined electrically so that, except for secondary carryover effects, a combined shear, moment, or torque bridge responded primarily to the shear, moment, or torque for the side of the tail on which the load was being measured. Final calibration equations using combined bridge outputs included carryover-effect corrections.

The combined strain-gage outputs were recorded on an 18-channel oscillograph with individual galvanometer responses flat to 60 cps. All data were evaluated by using nondimensional deflections as

$$\rho = \frac{\text{Flight deflection} - \text{Ground zero deflection}}{\text{Calibrate signal deflection}}$$

The sensitivity of each combined bridge was generally recorded prior to entering a maneuver through the use of a calibrate signal. With this system of data reduction, changes in battery voltage had no effect on the measurement of loads. In addition, galvanometer zeros with strain-gage power off were recorded to compensate for any mechanical shifts in the galvanometer zero position due to temperature effects in the recorder and any thermal electromotive-force effects in the strain-gage circuits.

Aerodynamic tail loads on the horizontal tail were obtained from the structural loads (measured by the strain-gage bridges) and the known tail weight and normal load factor from the equation

$$L_{t_{aero}} = L_{t_{struct}} - n_t W_t$$

The aerodynamic bending moments and torques were obtained in a similar manner.

The recorded data for all instruments were synchronized at 0.1-second intervals by means of a common timing circuit. All instruments were damped to about 0.67 of critical damping. A summary of pertinent quantities measured, instrument locations, and accuracies are given in the following table:

| Quantity | Location | Instrument range | Instrument accuracy |
|---|---|---|---|
| Normal acceleration, g units . . . . . . | 34.2 percent $\bar{c}$ | 0 to 2 | 0.005 |
| Normal acceleration, g units . . . . . . | 47.8 percent horizontal-tail root chord | -2 to 6 | 0.02 |
| Pitching acceleration, radians/sec$^2$ . . . | 25 percent $\bar{c}$ | ±0.50 | 0.01 |
| Dynamic pressure, lb/sq ft . . . . . . | 140 in. ahead of original nose | 0 to 800 | 1 |
| Static pressure, lb/sq ft . . . . . | 132 in. ahead of original nose | 0 to 2,200 | 2 |
| Tail shear, per side, lb . . . . . | Root of tail | ±25,000 | 60 |
| Tail torque, per side, in-lb . . . . | Root of tail | ±2,000,000 | 4,000 |

Tests

All tests were made with the airplane in the clean condition. The flight data evaluated in this report were taken from 68 push-down—pull-up maneuvers (the same maneuvers used in refs. 3 and 4) made at altitudes of 20,000, 25,000, 30,000, and 35,000 feet and an overall Mach number range from 0.427 to 0.812. The tests were made at normal and forward center-of-gravity positions and airplane weights ranging from 104,000 to 127,000 pounds. Table II is a summary of the flight conditions for these runs. In the table are listed the flight and run numbers, average Mach number, average dynamic pressure, test altitude, weight, and center-of-gravity position. The range of Mach number and dynamic-pressure changes during any test are also indicated. It might be noted that the center-of-gravity listings in table II differ slightly from those given for the same maneuvers in references 3 and 4. The airplane centers of gravity have been corrected for the effect of airplane attitude on the fuel-tank centers of gravity for the three large unbaffled fuselage tanks.

## METHODS AND RESULTS

The airplane pitching-moment parameters, that is, wing-fuselage aerodynamic-center position and zero-lift pitching-moment coefficient, and the airplane effective moment of inertia may be evaluated from flight measurements of the airplane motions and the horizontal-tail load. In appendix A, use is made of the airplane pitching-moment equation to set up two methods of analysis amenable to least-squares treatment. The methods are:

Method I.  A procedure in which direct tail-load measurements are used.

Method II.  A procedure in which elevator-angle measurements are used.

Pitching-moment parameters obtained by the use of either method include quasi-static wing-flexibility effects but the equations do not allow for dynamic wing, tail, or fuselage frequency-response effects since the bulk of the data presented was obtained without excitation of the major airplane components.

The following sections present the determination of the pitching-moment parameters from flight time-history data and comparisons with available wind-tunnel and mass-distribution data. The method used for extrapolating or correcting the measured aerodynamic-center positions to rigid-wing conditions is given in detail. The theoretical relationship existing between the measured or effective moment of inertia and the actual or rigid-airplane moment of inertia is also described.

### Basic Data

The least-squares data-reduction procedures as used for methods I and II are given in appendix B. These procedures are used for the evaluation of the required tail-load and elevator-angle coefficients for each of the 68 maneuvers studied. These tail-load and elevator-angle coefficients in turn are used for the evaluation of the airplane pitching-moment parameters. Both methods are illustrated by use of the time-history data for $n$, $\ddot{\theta}$, $\dot{\theta} l_t/V$, $L_{t_T}$, and $\delta$ shown in figures 2, 3, and 4 for an example maneuver (flight 12, run 27). The calculated tail-load and elevator-angle time histories from equations (B4) and (B6) are illustrated in figures 3 and 4, respectively.

It is demonstrated in appendix B that for method I a simplified form of equation (B2) which omits the $\dot{\theta} l_t/V$ term could be used for the

determination of the zero-lift tail load, the tail load per g, and the
tail load per unit pitching acceleration. The A, B, and C coeffi-
cients of equation (B2), along with their standard errors and errors of
fit, for each of the 68 maneuvers analyzed are given in table III.

The coefficients from the least-squares analysis of the elevator-
angle data (method II), along with their standard errors and errors of
fit, for each of the 68 maneuvers analyzed are given in table IV.

## Aerodynamic-Center Position

The B coefficients of method I and the $\partial \delta / \partial n$ coefficients of
method II, given in tables III and IV, respectively, as deduced from
flight time-history data now permit the determination of the wing-fuselage
aerodynamic-center location. This section illustrates the methods used to
extract the aerodynamic-center data and to extrapolate the data as meas-
ured for flexible-wing conditions to rigid-wing conditions. In appendix A,
equations (A8) and (A25) show the relationship between the aerodynamic-
center position d (the distance between airplane center of gravity and
wing-fuselage aerodynamic-center location) and the measured coefficients.
A general equation expressing the aerodynamic-center position in terms of
its location on the wing mean aerodynamic chord is

$$\left(X_{ac}\right)_{flex} = X_{cg} + \frac{d}{\bar{c}} 100 \tag{1}$$

and is used to correlate the data obtained at various center-of-gravity
locations.

Aerodynamic-center position using method I.- Equation (A8) of appen-
dix A gives the aerodynamic-center location d as

$$d = \frac{Bl_t}{W - B} \tag{2}$$

Inserting numerical values for the example maneuver of appendix B with
$B = 392$ (from eq. (B4)), $l_t = -552$ inches, and $W = 110,300$ pounds
in equation (2) gives

$$d = -1.97 \text{ inches}$$

The aerodynamic center in terms of the mean aerodynamic chord, using
equation (1) and the center-of-gravity position of 22.9 percent, thus
becomes

$$\left(X_{ac}\right)_{flex} = 22.9 + \left(\frac{-1.97}{1.559}\right) = 21.6 \text{ percent}$$

The error in $\left(X_{ac}\right)_{flex}$ may be determined by use of the standard error in the B coefficient as

$$\epsilon_{X_{ac}} \approx \frac{\epsilon_B l_t}{W - B} \frac{100}{\bar{c}} \tag{3}$$

Using the standard error of B from table III gives

$$\epsilon_{X_{ac}} = \pm \frac{358(-552)}{(109,910)(1.559)} = \pm 1.2 \text{ percent}$$

The aerodynamic-center positions and the associated standard errors for each of the 68 maneuvers are given in table V.

Aerodynamic-center position using method II.- Equation (A25) of appendix A gives the aerodynamic-center location d as

$$d = \frac{l_t \left(C_{L\alpha_t}\right)_f \left[\frac{\partial \delta}{\partial n} \frac{d\alpha_t}{d\delta} + \frac{di_t}{dn_t} + g \frac{l_t}{V^2} \frac{d\epsilon}{d\alpha} + \left(1 - \frac{d\epsilon}{d\alpha}\right)\frac{W}{a_F qS}\right] + \frac{\partial \delta}{\partial n} C_{m_\delta} \bar{c}_t}{\frac{W}{qS_t} - \left(C_{L\alpha_t}\right)_f \left[\frac{\partial \delta}{\partial n} \frac{d\alpha_t}{d\delta} + \frac{di_t}{dn_t} + g \frac{l_t}{V^2} \frac{d\epsilon}{d\alpha} + \left(1 - \frac{d\epsilon}{d\alpha}\right)\frac{W}{a_F qS}\right]} \tag{4}$$

For use in equation (4) values of the parameters $\left(C_{L\alpha_t}\right)_f$, $\frac{d\alpha_t}{d\delta}$, $\frac{d\epsilon}{d\alpha}$, and $C_{m_\delta}$ were obtained from reference 3 and the airplane lift-curve slope $a_F$ was obtained from reference 4. The parameter $\frac{di_t}{dn_t}$ (tail-incidence change due to fuselage bending under inertia loads) was obtained from equation (7) of reference 3. The remaining parameters required are g, the acceleration of gravity, V, the true airspeed, and q, the dynamic pressure. The quantity $\partial \delta/\partial n$ is the coefficient of equation (A19) associated with n and is given in table IV.

For the example maneuver, substitution of numerical values into equation (4) results in

$$d = -3.22 \text{ inches}$$

The aerodynamic center by method II for the example maneuver is from equation (1):

$$\left(X_{ac}\right)_{flex} = 22.9 + \left(\frac{-3.22}{1.559}\right) = 20.8 \text{ percent}$$

The error in $\left(X_{ac}\right)_{flex}$ may be computed from the standard error of the $\frac{\partial \delta}{\partial n}$ coefficient given in table IV as

$$\epsilon_{X_{ac}} = \frac{\left[l_t\left(C_{L_{\alpha_t}}\right)_f \frac{d\alpha_t}{d\delta} + C_{m_\delta}\bar{c}_t\right]\epsilon_{\partial\delta/\partial n}\frac{100}{\bar{c}}}{\frac{W}{qS_t} - \left(C_{L_{\alpha_t}}\right)_f\left[\frac{\partial\delta}{\partial n}\frac{d\alpha_t}{d\delta} + \frac{di_t}{dn_t} + g\frac{l_t}{v^2}\frac{d\epsilon}{d\alpha} + \left(1 - \frac{d\epsilon}{d\alpha}\right)\frac{W}{a_F qS}\right]} \quad (5)$$

Using the standard error of $\partial\delta/\partial n$ from table IV gives

$$\epsilon_{X_{ac}} = \frac{\left[(-552)(0.0559)(0.420) + (-0.0086)103\right](\pm 0.258)}{1.559(2.562)} = \pm 0.9 \text{ percent}$$

The aerodynamic-center positions and their associated standard errors for all 68 maneuvers are given in table V where they may be compared with the values determined by using method I.

Extrapolation to rigid-wing conditions.- The aerodynamic-center-position data in table V are for flexible-wing conditions. If the effects of wing flexibility are known, the flight measurements may be extrapolated to rigid-wing conditions and the variation of aerodynamic-center position with Mach number established. Data are available in reference 5 which may be used for this extrapolation. The forward shift of the wing aerodynamic-center position as a function of the flexibility parameter $qm_R$ is shown in figure 5, as determined from the theoretical curve (for an average value of $W = 110,000$ pounds) of figure 4(c) in reference 5 by conversion of the root center-of-pressure variation with $qm_R$ to percent mean aerodynamic chord. Since the wing additional-load center-of-pressure data in figure 4(c) of reference 5 were determined from wing-root aerodynamic torques and the airplane center-line shear $\left(\frac{1}{2}nW - \frac{1}{2}L_t\right)$, the rigid-wing—fuselage aerodynamic-center position may be determined from the equation

$$\left(X_{ac}\right)_r = \left(X_{ac}\right)_{flex} + \Delta X_{ac} \qquad (6)$$

When equation (6) is used it is assumed that the wing-fuselage aerodynamic-center position differs from the wing aerodynamic-center position only by a constant for any given Mach number and that changes in dynamic pressure do not affect the fuselage contribution to the total wing-fuselage aerodynamic-center position.

The values of $q m_R$ for use in the determination of $\Delta X_{ac}$ from figure 5 are listed in table V and were obtained from the dynamic pressures given in table II and the rigid-wing—fuselage lift-curve slopes $m_R$ given in reference 4. The $\left(X_{ac}\right)_r$ values obtained from equation (6) for the method I and method II data and the $\Delta X_{ac}$ values from figure 5 are given in table V. The values of $\left(X_{ac}\right)_r$ for both methods are plotted in figure 6 and are identified by method.

It will be noted that the errors associated with the aerodynamic centers $\epsilon_{X_{ac}}$ of table V are not constant. Use was made of these errors to define weighting factors to obtain weighted average values of aerodynamic center at the group Mach numbers indicated in table V. The weighting factor is defined as

$$w = \left(\frac{1}{\epsilon_{X_{ac}}}\right)^2 \qquad (7)$$

and the weighted average aerodynamic-center position is defined by the equation

$$\left(\bar{X}_{ac}\right)_r = \frac{\sum w\left(X_{ac}\right)_r}{\sum w} \qquad (8)$$

The standard error of the weighted average is given by the equation

$$\epsilon_{\bar{X}_{ac}} = \sqrt{\frac{\sum w\left(X_{ac}\right)_r^2 - \left(\bar{X}_{ac}\right)_r \sum w\left(X_{ac}\right)_r}{N \sum w}} \qquad (9)$$

The last column of table V gives the weighted average values of the aerodynamic-center position and the standard errors computed using equations (8) and (9) for the Mach number groups used. These weighted average

aerodynamic-center values are also plotted as circles in figure 7 with a line faired through the data to indicate a reasonable variation with Mach number, the standard error of each point (shown as the vertical lines within the Symbols) being considered.

Comparison with wind-tunnel data.- Wind-tunnel model data corrected for model flexibility effects are given in reference 7 on pages L-124, L-126, and L-128. From these data the wing-fuselage aerodynamic-center data shown in figure 7 (the diamond-shaped symbols) were obtained for the available Mach numbers and may be compared with the flight measurements.

Aerodynamic-center positions at various altitudes.- The wing-fuselage aerodynamic-center position as affected by wing flexibility may be calculated for various altitudes by the use of equation (6), the $\Delta X_{ac}$ data of figure 5, and the faired curve of figure 7. The results of these calculations are shown in figure 8 and are considered to be the best estimates of aerodynamic-center position that can be made from the flight data. The results are limited to a low Mach number of 0.40, a high $qm_R$ of 50, and an airplane weight range from 110,000 to 130,000 pounds since these conditions represent the limits within which the flight measurements were obtained.

## Zero-Lift Pitching-Moment Coefficient

In the following section the determination of the zero-lift wing-fuselage pitching-moment coefficients from the A coefficient of equation (B2) (for method I) and from the $\delta_0$ coefficient of equation (B5) (for method II) is illustrated with results presented for both methods.

Method I.- Equation (A9) of the appendix is used to determine the wing-fuselage zero-lift pitching-moment coefficient as

$$C_{m_{O_M}} = -\frac{Ax_t}{qS\bar{c}} \tag{10}$$

where

$$x_t = l_t + d \tag{11}$$

For the example maneuver (flight 12, run 27), the substitution into equation (10) of numerical values for A from equation (B4) and

$$x_t = (-552) + (-1.97) = -554 \text{ inches}$$

produces a measured $C_{m_{O_M}}$ value equal to

$$C_{m_{O_M}} = -\frac{(-1702)(-554)}{(159)(1428)(155.9)} = -0.0266$$

The values of $C_{m_{O_M}}$ thus obtained from the A coefficients of table III and the use of equations (10) and (11) are given in table VI and are plotted as a function of Mach number in figure 9 for each of the 68 maneuvers. It was demonstrated in reference 3, however, that the measured tail loads were subject to large zero shifts (ranging from 16,000 to -6,000 pounds). In order to correct the measured zero-lift tail load, use is made of the equation

$$A_{corr} = A - Z' - \frac{Z_T}{x_t} \tag{12}$$

where $Z'$ is the zero shift in measured tail load given in table III of reference 3 for the same maneuvers used in the present analysis and $Z_T$ is the zero shift in tail aerodynamic torque determined from a tail torque and tail angle-of-attack analysis similar to that used for the tail loads in reference 3. For the example maneuver, use of equation (12) gives

$$A_{corr} = -1702 - (20) - (240) = -1962$$

The zero-lift wing-fuselage pitching-moment coefficient is then recalculated by use of the equation

$$C_{m_O} = \frac{-A_{corr}\, x_t}{qS\bar{c}} \tag{13}$$

which with numerical values inserted becomes

$$C_{m_O} = \frac{-(-1962)(-554)}{(159)(222625)} = -0.0307$$

for the example maneuver. The error in $C_{m_O}$ may be estimated by the use of the standard error in the A coefficient as

$$\epsilon C_{m_{O_I}} = \frac{\epsilon_A x_t}{qS\bar{c}} \tag{14}$$

Using the standard error of A from table III gives

$$\epsilon C_{m_{O_I}} = \frac{(\pm 363)(554)}{(159)(222625)} = \pm 0.0057$$

The corrected zero-lift wing-fuselage pitching-moment coefficients and
their associated errors are listed in table VI.  Figure 10 is a plot of
the  $C_{m_O}$  values as a function of Mach number and, although scatter does
still exist, these results are a decided improvement over the results pre-
sented in figure 9.

Method II.- The elevator-angle type of solution may be used to deter-
mine the zero-lift wing-fuselage pitching-moment coefficients, as illus-
trated by equation (A24) of the appendix:

$$C_{m_{O_{II}}} = -\frac{S_t x_t}{S\bar{c}} \left\{ \delta_O \left[ \left(C_{L_{\alpha_t}}\right)_f \frac{d\alpha_t}{d\delta} + C_{m_\delta} \frac{\bar{c}_t}{x_t} \right] - \right.$$

$$\left. \left(C_{L_{\alpha_t}}\right)_f \left[ 3.00 + g \frac{l_t}{V^2} \frac{d\epsilon}{d\alpha} - \left(1 - \frac{d\epsilon}{d\alpha}\right)\left(\alpha_{O_{adj}} + 2.75\right) \right] \right\} \qquad (15)$$

The substitution of numerical values for the example maneuver, using the
$\delta_O$  value of table IV, geometric parameters, and tail angle-of-attack
parameters from reference 3, results in

$$C_{m_{O_{II}}} = -0.0326$$

with an associated error of ±0.0033.  Values of  $C_{m_{O_{II}}}$  and their standard
errors are listed in table VI.  Figure 11 is a plot of the  $C_{m_{O_{II}}}$  values
as a function of Mach number, which is seen to indicate (although with
somewhat more scatter) the same average variation with Mach number as
illustrated in figure 10 for the method I data.

The correlation between these two methods of evaluating zero-lift
wing-fuselage pitching-moment data is seen more clearly in figure 12
where  $C_{m_{O_I}}$  is plotted against  $C_{m_{O_{II}}}$.  The solid line in this figure
is the perfect agreement line and the dashed sidebands represent an
average departure from agreement based on the average of the errors
listed in table VI for each method.  With a few exceptions most of the
data lie reasonably close to the correlation line.

Variation with Mach number.- The  $C_{m_O}$  data of figures 10 and 11
indicated a tendency for the lower altitude data to have smaller absolute
values of  $C_{m_O}$.  This trend is in agreement with theory since increasing
the dynamic pressure at constant Mach number relieves both the bending
and torsional moments associated with the zero-lift wing loads and thus
reduces the wing contribution to  $C_{m_O}$.  Theoretical calculations indicate,

however, that for the maximum $q_{m_R}$ of the present tests the change in $C_{m_O}$ would be only 0.0010. Other factors not specifically corrected for in either set of $C_{m_O}$ data are the pitching-moment coefficient due to tail drag which was estimated to have a maximum value of 0.0023 and the pitching-moment coefficient due to engine thrust which was estimated to vary from 0.0019 to 0.0014 for the dynamic pressure range of the 68 maneuvers used in the analysis.

In order to determine a more definite variation of $C_{m_O}$ with Mach number, the data shown in figures 10 and 11 were used to determine weighted average values of $C_{m_O}$ at each of the Mach number groups shown in table VI. The weights were assigned by use of a weighting factor $w$ similar to that given in equation (7) except that $\epsilon_{x_{ac}}$ was replaced by $\epsilon_{C_{m_O}}$. The weighted average $C_{m_O}$ is given by the equation

$$\overline{C_{m_O}} = \frac{\sum wC_{m_O}}{\sum w} \tag{16}$$

and the standard error of the weighted average is given by the equation

$$\overline{\epsilon_{C_{m_O}}} = \sqrt{\frac{\sum w\left(C_{m_O}\right)^2 - \overline{C_{m_O}} \sum wC_{m_O}}{n \sum w}} \tag{17}$$

The results of the application of equations (16) and (17) to the data for each of the Mach number groups are given in table VI and plotted in figure 13 as a function of Mach number.

Comparison with wind-tunnel data.- Wind-tunnel data corrected for model flexibility effects are given in reference 7 on pages L-124, L-126, and L-128. From these data the wing-fuselage zero-lift pitching-moment coefficients (shown as the diamond symbols in fig. 13) were obtained.

Pitching Moment of Inertia and Radius of Gyration

In the following sections the effects of wing flexibility on the measured and calculated effective airplane moments of inertia are presented.

$k_{y_f}^2$ from theory.- The effective moment of inertia of the airplane including the effects of wing flexibility is defined by equation (A10) as

$$I_{y_f} = I_y - d_{\ddot{\theta}} \frac{dL_w}{d\ddot{\theta}} \tag{18}$$

The values of $dL_w/d\ddot{\theta}$ and $d_{\ddot{\theta}}$ to be used in equation (18) are difficult to determine by direct experimentation and recourse is made here to estimating them by theoretical means. The aerodynamic wing load due to pitching acceleration $dL_w/d\ddot{\theta}$ and the associated chordwise center of pressure $d_{\ddot{\theta}}$ were computed by the superposition method of reference 8 as modified and used in references 4 and 5. The results of these computations are shown in figure 14 where the load (in this case for both wings) and the center of pressure (given in terms of percent M.A.C.) are plotted as functions of the flexibility parameter $qm_R$. The relationship between the ordinate $X_{\ddot{\theta}}$ of figure 14(a) and the center of pressure $d_{\ddot{\theta}}$ is given by the equation

$$d_{\ddot{\theta}} = \left(X_{ac} - X_{\ddot{\theta}}\right)\frac{\bar{c}}{100} \tag{19}$$

where $X_{ac}$ may be found from figure 8. The substitution of equation (19) into equation (18) and division by $W/g$ produces the following equation for effective radius of gyration squared:

$$k_{y_f}{}^2 = k_y{}^2 - \frac{g}{W}\left[\left(X_{ac} - X_{\ddot{\theta}}\right)\frac{\bar{c}}{100}\frac{dL_w}{d\ddot{\theta}}\right] \tag{20}$$

It was found that in the range of interest of $qm_R$ for the present tests the product $\left(X_{ac} - X_{\ddot{\theta}}\right)\frac{dL_w}{d\ddot{\theta}}$ was approximately linear and was equal to

$$\left(X_{ac} - X_{\ddot{\theta}}\right)\frac{dL_w}{d\ddot{\theta}} = 10{,}000qm_R \tag{21}$$

Thus, $k_{y_f}{}^2$ in units of square feet is given by the equation

$$k_{y_f}{}^2 = k_y{}^2 - \frac{32.2 \times 1.559}{12W}10{,}000qm_R$$

$$k_{y_f}{}^2 = k_y{}^2 - 42{,}000 \frac{qm_R}{W} \tag{22}$$

Values of $k_{y_f}{}^2$ calculated by equation (22) are given in table VII and are plotted in figure 15 as a function of $qm_R/W$ for the 68 test maneuvers. In the calculation of $k_y{}^2$ the empty-weight moment of inertia

given in reference 9 for a ground determination of $I_y$ for the test airplane of 933,000 slug-feet$^2$ was used along with the fuel weights and locations.

$k_{y_f}^2$ from flight data.- The squared values of radius of gyration, obtained by use of method I and method II flight data and equations (A10) and (A26) of the appendix (along with their standard errors), are given in table VII for all maneuvers. The average values of $k_{y_f}^2$ (from methods I and II) are also given in table VII and plotted in figure 15. It will be noted that the measured $k_{y_f}^2$ values have more scatter but a greater mean variation with $qm_R$ than the calculated values. The disagreement between measured and calculated $k_y^2$ values may be due to actual differences in the rigid-wing values or an incorrect theoretical variation with $qm_R$. In order to allow for these differences, the following procedure was used to correlate flight and calculated values of $k_{y_f}^2$. If the values of $k_{y_f}^2$ are assumed to be linear with respect to $qm_R$, the following equations may be written:

$$\left(k_{y_f}^2\right)_{calc} = \left(k_y^2 + \epsilon_1\right) + \frac{\left(dk_{y_f}^2\right)_{calc}}{d\frac{qm_R}{W}}\frac{qm_R}{W} \tag{23}$$

$$\left(k_{y_f}^2\right)_{meas} = \left(k_y^2 + \epsilon_2\right) + \frac{\left(dk_{y_f}^2\right)_{meas}}{d\frac{qm_R}{W}}\frac{qm_R}{W} \tag{24}$$

Subtracting equation (23) from equation (24) results in the following equation for $\Delta k_{y_f}^2$:

$$\Delta k_{y_f}^2 = \left(k_{y_f}^2\right)_{meas} - \left(k_{y_f}^2\right)_{calc}$$

$$= \left(\epsilon_2 - \epsilon_1\right) + \left[\frac{\left(dk_{y_f}^2\right)_{meas}}{d\frac{qm_R}{W}} - \frac{\left(dk_{y_f}^2\right)_{calc}}{d\frac{qm_R}{W}}\right]\frac{qm_R}{W} \tag{25}$$

Equation (25) now permits the correlation of all the data as a function of $qm_R$ since the actual $k_y^2$ values that differ from run to run because of weight-distribution differences have been eliminated by the subtraction. Columns of $\Delta k_{y_f}^2$ values and $\frac{qm_R}{W}$ are shown in table VII. A least-squares procedure was used with the data to establish the following relationship between $\Delta k_{y_f}^2$ and $qm_R/W$:

$$\Delta k_{y_f}^2 = (6.6 \pm 5.3) - (11.5 \pm 2.6)\left(\frac{qm_R}{W} \times 10^4\right) \tag{26}$$

Since the standard error of the value $(\epsilon_2 - \epsilon_1)$ of equation (26) is $\pm 5.3$ and the average standard error in the measured $k_{y_f}^2$ from table VII is $\pm 5.8$, the conclusion to be reached is that the flight measurements agree with the calculated values of $k_y^2$ for rigid-wing conditions. The difference between the measured and calculated $k_{y_f}^2$ values is in the variation with $\frac{qm_R}{W}$. The equation which represents the flexible-wing effective radius of gyration is, thus, from equations (26), (25), and (22):

$$k_{y_f}^2 = k_y^2 - (115,000 \pm 26,000 + 42,000)\frac{qm_R}{W}$$

or

$$k_{y_f}^2 = k_y^2 - (157,000 \pm 26,000)\frac{qm_R}{W} \tag{27}$$

$\underline{k_{y_f}^2 \text{ from wing-twist data.-}}$ The differences between the measured and calculated variations of $k_{y_f}^2$ with $qm_R/W$ were sufficiently large to require some further evidence or confirmation. In figure 15 of reference 2, optigraph measurements for the test airplane were reported which showed a considerable disagreement between measured and calculated values of wing twist associated with pitching accelerations. These twists as plotted in figure 15 of reference 2 are not those due to pitching inertia alone but include an additional air load component. After correction for this component, the aerodynamic load distribution due to twist resulting from pitching inertia was computed by use of the method of reference 10 for the example of figure 15 in reference 2. Integration of the resulting load distribution for both wings gave a load per unit pitching acceleration of -15,040 pounds with a center of pressure at 86.9 percent $\bar{c}$. Both of these points are indicated on the theoretical curves presented in

figure 14. Equation (20) was then used to compute the effective radius of gyration squared as

$$k_{y_f}{}^2 = 358.35 - \frac{386(1.559)}{144(108,000)}\Big[(18.8 - 86.9)(-15,040)\Big]$$

$$= 318.52 \text{ feet}^2$$

where 358.35 was the rigid value of $k_y{}^2$ and 108,000 was the weight for the conditions of the data of reference 2. The value of $qm_R$ for this example is 19.6; thus, the application of equation (27) results in

$$k_{y_f}{}^2 = 358.35 - \frac{157,000}{108,000} 19.6$$

$$= 329.86 \text{ feet}^2$$

The theoretical value is determined from equation (22) as 350.73 feet$^2$.

The following table indicates the correlation between the various methods of determining the effective radius of gyration squared for the test airplane under the average conditions used:

| Method | $k_{y_f}{}^2$, ft$^2$ | $\epsilon_{k_{y_f}}{}^2$, ft$^2$ |
|---|---|---|
| Theoretical (eq. (22)) . . . . . . . . . . . . . . . . . | 350.73 | ----- |
| Analysis of all 68 flight maneuvers (eq. (27)) . . . | 329.86 | ±4.72 |
| Wing-twist measurements . . . . . . . . . . . . . . | 318.52 | ----- |

Better agreement is seen to exist between the $k_{y_f}{}^2$ value using wing-twist measurements and the value determined by use of equation (27) than for the theoretical value determined by use of equation (22).

## DISCUSSION

The preceding sections of the report have presented the results of the analyses and comparisons with theory and available wind-tunnel data as well as details of the analytical methods used to evaluate the flight

data.  The following discussion concerns the importance of the many fac-
tors included or omitted in the present analysis.

It is possible to lose sight of the importance of the supporting
experimental studies necessary for the analysis of the horizontal-tail
loads on a large flexible swept-wing aircraft.  Although the present
analysis was complicated by some difficulties, which were unforeseen
when the flight-test program was originally laid out, the detailed sup-
porting instrumentation which measured airplane angle of attack, wing
deflection and twist, and fuselage deflection proved to be invaluable in
many phases of the data analysis.  In brief, the determination of the
rigid wing-fuselage aerodynamic-center position from the flight data was
considerably simplified as a result of the flight measurements of wing
center of pressure presented in reference 5.

The determination of wing-fuselage zero-lift pitching-moment coef-
ficients from the flight data, which included large zero shifts, was only
possible as a result of the tail-load analysis presented in reference 3
which required the wing-lift-curve slope and angle-of-zero-lift data pre-
sented in reference 4.  A major factor in rationalizing the tail loads as
functions of angle of attack and elevator angle was the availability of
flight measurements of fuselage deflections which have since been reported
in reference 11.

The evaluation of the effects of wing flexibility on the effective
moment of inertia was aided by the theoretical studies used in refer-
ences 1, 2, 4, and 5, the basic moment-of-inertia data provided by refer-
ence 9, and the supporting check information obtained from the wing-twist
measurements reported in reference 2.

The analysis of elevator-angle-deflection time-history data used in
the present report to confirm the direct tail-load evaluation of
aerodynamic-center position, zero-lift wing-fuselage pitching-moment
coefficient, and effective airplane moment of inertia was based directly
on the analysis of references 3 and 4.


Basic-Data Coefficients

When method I was used to fit the tail-load time-history data,
it was found that the wing-fuselage pitching moment due to pitching
velocity produced immeasurably small horizontal tail loads.  A theoretical
calculation of the tail load per unit $\dfrac{\dot{\theta} l_t}{V}$ (as used in the airplane
pitching-moment equation (A1), not the tail-load—angle-of-attack equa-
tion (A15)) for the example maneuver (flight 12, run 27) resulted in

$$\frac{dL_{t_T}}{d\,\dfrac{\dot{\theta}l_t}{V}} = -18.0 \text{ pounds per degree}$$

which may be compared with the discarded value of $\dfrac{dL_{t_T}}{d\,\dfrac{\dot{\theta}l_t}{V}} = 82$ pounds

per degree noted for this maneuver in the flight analysis equation (B3).

The equations used to fit the tail-load and elevator-angle time-history data (eqs. (B2) and (B5)) did not allow for the effects of dynamic wing and fuselage flexibility and, yet, no discernible differences were found in comparing the coefficients of the slow-rate and fast-rate maneuvers. In several cases, dynamic wing-flexibility effects were suspected and the use of wing-tip flapping accelerations improved the fit to the time-history data without altering the primary coefficients. It was felt, therefore, that reasonably accurate results were thus obtained for the bulk of the data analyzed.

A factor somewhat more difficult to define positively is the linearity of the wing-fuselage pitching-moment coefficient with normal-force coefficient. The forms of the equations used force linearity and, for some of the higher altitude data where results were obtained at relatively high normal-force coefficients, this may have resulted in erroneous slopes and intercepts. All suspected departures from linearity were checked by the error-distribution time histories.

Another probable source of error was the sloshing motion of the fuel in the three large unbaffled fuselage fuel tanks, which may have introduced errors in the assumed equation of airplane motion.

Aerodynamic-Center Position

Aside from the factors previously mentioned the accuracy with which the in-flight center-of-gravity position could be determined governs the accuracy of the flight values of wing-fuselage aerodynamic-center position. Corrections were made to account for the effect of airplane attitude on the fuel level and the resultant effect on center-of-gravity position. However, there was some indication from ground tests that the fuel-gage readings were not entirely independent of airplane attitude. The agreement shown between the aerodynamic-center positions determined by methods I and II is excellent and with few exceptions well within their calculated standard errors. The agreement between the data for the rigid-wing aerodynamic-center position shown in figure 7 and the wind-tunnel data seems reasonable. In the Mach number range from 0.70 to 0.775 there is a difference of only $0.01\bar{c}$. The rearward shift of

aerodynamic-center position indicated above a Mach number of about 0.78 is believed to be associated with the fuselage since the wing aerodynamic-center position given in reference 5 remains at roughly 23.4 percent of the local wing chord up to $M = 0.81$.

## Zero-Lift Pitching-Moment Coefficient

The agreement between the corrected zero-lift pitching-moment coefficients measured by use of method I and those measured by use of method II indicated that the tail-load zero-shift correction method proposed in reference 3 was theoretically and practically sound. The differences between the flight values of $C_{m_0}$ shown in figure 13 and the wind-tunnel values (ref. 7) are large and not easily explainable.

A source of error in the determination of $C_{m_0}$ from flight data by use of either method I or method II is the accuracy of the elevator-angle measurement. While, for the present tests, the elevator-angle data were repeatable to within ±0.1 degree for comparable flight conditions, an error in $C_{m_0}$ due to elevator-angle zero errors $\left(\epsilon_{C_{m_{0\delta}}}\right)$ would be approximately equal to

$$\epsilon_{C_{m_{0\delta}}} \approx 0.68 C_{L_\delta} \epsilon_\delta$$

which with a maximum value of $C_{L_\delta}$ from reference 4 as 0.03 would be

$$\epsilon_{C_{m_{0\delta}}} \approx 0.02 \epsilon_\delta$$

As detailed in the section entitled "Methods and Results," the neglect of the effects of wing twist, tail drag, and pitching moment due to engine thrust could produce a maximum error in the flight measurements of $C_{m_0}$ of +0.0052.

## Moment of Inertia and Radius of Gyration

The major factor affecting the accuracy of the determination of $I_{y_f}$ or $k_{y_f}^2$ for any individual maneuver is believed to be the effect of fuel sloshing on the airplane motion. In some abrupt maneuvers during which the tail of the airplane accelerated from positive to negative g and back again, the fuel in the rear tank slammed back to the bottom of the tank and, as a result, produced considerable vibration in accelerometer

readings at the center of gravity. Although an attempt was made to elimi-
nate portions of the maneuvers from the analysis when such occurred, the
large surging actions of the fuel undoubtedly have contributed to some
of the scatter in the $I_y$ data.

The good agreement between the measured and calculated values of
$k_y{}^2$ for the rigid wing is believed to be indicative of the overall accu-
racy of the methods used to extract the airplane static stability param-
eters from the flight tail-load and elevator-angle measurements.

The variation shown between theory and experiment in the changes
of $\dot{k}_{y_f}{}^2$ with the flexibility parameter $qm_R/W$ is puzzling even though
it has been confirmed qualitatively by the wing-twist measurements of
reference 2. This disagreement may be associated with unaccounted for
local wing-section distortions near the tip or wing twists associated
with dynamic motions of the wing tip which may be closely phased with
the pitching acceleration time history.

## CONCLUDING REMARKS

Flight measurements of wing-fuselage aerodynamic-center position,
zero-lift pitching-moment coefficient, and effective airplane moment of
inertia have been presented as derived from the analysis of 68 push-pull
maneuvers on a large flexible swept-wing airplane in a Mach number range
from 0.42 to 0.81 at pressure altitudes from 20,000 to 35,000 feet. The
parameters as derived by two methods from measured horizontal-tail loads
and elevator angles were in excellent agreement. The method for cor-
recting for tail-load zero shifts (proposed in NACA RM L56J02) was applied
to the flight data with good results, as evidenced by a comparison of the
uncorrected and corrected zero-lift pitching-moment coefficients derived
from the tail-load measurements.

The effects of wing flexibility on the aerodynamic-center position
and on the zero-lift pitching-moment coefficient were predictable by
theory. The relief provided by the wing bending and twisting due to
pitching-acceleration inertia loads to the effective moment of inertia
was not predictable by theory. For the one check case available, essen-
tial agreement was obtained between optigraph data and tail-load data
for the relief due to pitching-acceleration wing loads.

Specifically for the test airplane it was found that:

1. Reasonable agreement was obtained between flight-measured rigid-
wing—fuselage aerodynamic-center positions and those determined from
wind-tunnel tests.

2. The rigid-wing—fuselage aerodynamic-center position was constant at 24.4 percent mean aerodynamic chord up to a Mach number of 0.78, after which it shifted rearward as the Mach number increased to its maximum flight value of 0.81.

3. The rearward shift in the wing-fuselage aerodynamic center above a Mach number of 0.78 appeared to be associated with the fuselage since the wing aerodynamic-center position given in NACA RM L57E28 remained constant at 23.4 percent of the local wing chord up to a Mach number of 0.81.

4. There were large differences between the wind-tunnel and flight-determined values of zero-lift wing-fuselage pitching-moment coefficient over the complete Mach number range of the tests.

5. The moments of inertia determined from the flight measurements agreed with calculated values for the rigid-wing case.

6. Calculated effective moments of inertia, which included the relief due to wing bending due to pitching-acceleration inertia loads, did not agree with those measured by the present flight tests.

7. For the test airplane, the pitching moment due to pitching-velocity loads on the wing was shown to be insignificant both theoretically and from the tail-load measurements.


Langley Aeronautical Laboratory,
       National Advisory Committee for Aeronautics,
              Langley Field, Va., August 1, 1957.

# APPENDIX A

## PITCHING-MOMENT EQUATIONS

The pitching moments on the airplane may be expressed by taking the summation of the moments about the wing-fuselage aerodynamic-center location as

$$\sum M_{ac} = 0 = -nWd + C_{m_0}qS\bar{c} - I_y\ddot{\theta} + L_{\ddot{\theta}}\,d\ddot{\theta} + L_{\dot{\theta}}\,d\dot{\theta} + L_t x_t + C_{m_\delta}\delta qS_t\bar{c}_t \tag{A1}$$

In equation (A1) positive forces act upwards, positive moments are nose up, and distances rearward of the aerodynamic center are negative.

The parameters in equation (A1) which are functions of the wing flexibility are the aerodynamic-center location $d$, the wing-fuselage zero-lift pitching-moment coefficient $C_{m_0}$, the lift on the wing due to the load induced by wing deflection due to pitching inertia $L_{\ddot{\theta}}$, and the lift on the wing due to the distribution of lift due to pitching velocity $L_{\dot{\theta}}$. The term $L_{\ddot{\theta}}$ is defined as

$$L_{\ddot{\theta}} = \frac{dL_W}{d\ddot{\theta}}\,\ddot{\theta} \tag{A2}$$

and the term $L_{\dot{\theta}}$ is defined as

$$L_{\dot{\theta}} = \frac{dL_W}{d\,\dfrac{\dot{\theta}l_t}{V}}\,\frac{\dot{\theta}l_t}{V} \tag{A3}$$

### Method I – Direct Tail-Load Measurement

Equation (A1) may be written as

$$L_t x_t + C_{m_\delta}\delta qS_t\bar{c}_t = -C_{m_0}qS\bar{c} + nWd + \left(I_y - \frac{dL_W}{d\ddot{\theta}}\,d\ddot{\theta}\right)\ddot{\theta} - \frac{dL_W}{d\,\dfrac{\dot{\theta}l_t}{V}}\,d\dot{\theta}\,\frac{\dot{\theta}l_t}{V} \tag{A4}$$

For the test data analyzed in the present report, the horizontal-tail
aerodynamic load $L_t$ and the tail aerodynamic torque

$$T_t = C_{m_\delta} \delta q S_t \bar{c}_t \tag{A5}$$

were both measured by means of strain gages; thus, equation (A4) may be
used as

$$L_{t_T} = L_t + \frac{T_t}{x_t} = \frac{-C_{m_0} q S \bar{c}}{x_t} + \frac{nWd}{x_t} + \left( I_y - \frac{dL_w}{d\ddot{\theta}} d_{\ddot{\theta}} \right) \frac{\ddot{\theta}}{x_t} - \frac{dL_w}{d\frac{\dot{\theta} l_t}{V}} \frac{d_{\dot{\theta}}}{x_t} \frac{\dot{\theta} l_t}{V} \tag{A6}$$

In a form simplified for least-squares analysis, equation (A6) may be
written as

$$L_{t_T} = A + Bn + C\ddot{\theta} + D\frac{\dot{\theta} l_t}{V} \tag{A7}$$

From the coefficients $A$, $B$, $C$, and $D$ of equation (A7) and the corre-
sponding terms of equation (A6), the pitching-moment parameters of inter-
est may be defined as aerodynamic-center location $d$

$$d = \frac{B l_t}{W - B} \tag{A8}$$

zero-lift pitching-moment coefficient $C_{m_0}$

$$C_{m_0} = -\frac{A x_t}{q S \bar{c}} \tag{A9}$$

effective airplane moment of inertia $I_{y_f}$

$$I_{y_f} = I_y - \frac{dL_w}{d\ddot{\theta}} d_{\ddot{\theta}} = C x_t \tag{A10}$$

and the pitching moment due to pitching velocity $L_{\dot{\theta}} d_{\dot{\theta}}$

$$L_{\dot{\theta}} d_{\dot{\theta}} = D \frac{\dot{\theta} l_t}{V} x_t \tag{A11}$$

Method II - Pitching-Moment Parameters From

Elevator-Angle Measurements

For the determination of pitching-moment parameters from elevator-angle measurements, a more complicated series of equations must be written which also include the effect of fuselage deflection on the horizontal-tail angle of attack. Equation (A1) is rewritten as

$$L_t = -C_{m_0} \frac{qS\bar{c}}{x_t} + \frac{nWd}{x_t} + \left(\frac{I_y}{x_t} - \frac{dL_w}{d\ddot{\theta}} \frac{d\ddot{\theta}}{x_t}\right)\ddot{\theta} - \left(\frac{C_{m_\delta}\delta qS_t\bar{c}_t}{x_t}\right) - \frac{dL_w}{d\frac{\dot{\theta}l_t}{V}} \frac{d\dot{\theta}}{x_t} \frac{\dot{\theta}l_t}{V} \quad (A12)$$

Now

$$L_t = C_{L_{\alpha_t}} qS_t \alpha_t \quad (A13)$$

and $\alpha_t$ can be written specifically for the test airplane by using equations (4) and (6) of reference 3:

$$\alpha_t = -3.00 + \alpha_w\left(1 - \frac{d\epsilon}{d\alpha}\right) - \frac{\dot{\theta}l_t}{V} \frac{d\epsilon}{d\alpha} + g \frac{(n-1)}{V^2} l_t \frac{d\epsilon}{d\alpha} - \frac{\dot{\theta}l_t}{V} +$$

$$\frac{d\alpha_t}{d\delta} \delta + \frac{di_t}{dn_t} n_t + \frac{di_t}{dL_t} L_t \quad (A14)$$

By the substitution of equation (A14) into (A13) and factoring out the tail-load terms, the tail-load equation may be rewritten as

$$L_t = \frac{C_{L_{\alpha_t}} qS_t}{1 - \frac{di_t}{dL_t} C_{L_{\alpha_t}} qS_t}\left[-3.00 + \alpha_w\left(1 - \frac{d\epsilon}{d\alpha}\right) + \frac{d\alpha_t}{d\delta} \delta - \frac{\dot{\theta}l_t}{V}\left(1 + \frac{d\epsilon}{d\alpha}\right) + \right.$$

$$\left. g \frac{l_t}{V^2} \frac{d\epsilon}{d\alpha}(n-1) + \frac{di_t}{dn_t} n_t\right] \quad (A15)$$

Hereafter, the expression $\dfrac{C_{L_{\alpha_t}}}{1 - \dfrac{di_t}{dL_t} C_{L_{\alpha_t}} qS_t}$ is defined as the effective

tail-lift-curve slope $\left(C_{L_{\alpha_t}}\right)_f$.

With the use of the additional equations

$$n_t = n - 1.352\ddot{\theta} \tag{A16}$$

$$\alpha_w = \alpha_{0_{adj}} + \frac{1}{a_F} C_{N_{AC}} + i_w \tag{A17}$$

$$C_{N_{AC}} = \frac{nW}{qS} - \frac{I_{y_f}\ddot{\theta}}{x_t Sq} \tag{A18}$$

where equation (A16) is the tail load factor expressed in terms of the center-of-gravity normal load factor and pitching acceleration and equations (A17) and (A18) are used in reference 3 to define the wing angle of attack, equations (A15) and (A12) can be combined to give

$$\delta = \delta_0 + \frac{\partial\delta}{\partial\frac{\dot{\theta}l_t}{V}}\frac{\dot{\theta}l_t}{V} + \frac{\partial\delta}{\partial n}n + \frac{\partial\delta}{\partial\ddot{\theta}}\ddot{\theta} \tag{A19}$$

where

$$\frac{\partial\delta}{\partial\frac{\dot{\theta}l_t}{V}} = \frac{\left[\left(1 + \frac{d\epsilon}{d\alpha}\right)\left(C_{L_{\alpha_t}}\right)_f - \frac{dL_w}{d\frac{\dot{\theta}l_t}{V}}\frac{d\dot{\theta}}{x_t q S_t}\right]}{\left[\left(C_{L_{\alpha_t}}\right)_f \frac{d\alpha_t}{d\delta} + C_{m_\delta}\frac{\bar{c}_t}{x_t}\right]} \tag{A20}$$

$$\delta_0 = \frac{-C_{m_0}\frac{S\bar{c}}{S_t x_t} + \left(3.00 + g\frac{l_t}{V^2}\frac{d\epsilon}{d\alpha}\right)\left(C_{L_{\alpha_t}}\right)_f - \left(1 - \frac{d\epsilon}{d\alpha}\right)\left(C_{L_{\alpha_t}}\right)_f\left(\alpha_{0_{adj}} + i_w\right)}{\left[\left(C_{L_{\alpha_t}}\right)_f \frac{d\alpha_t}{d\delta} + C_{m_\delta}\frac{\bar{c}_t}{x_t}\right]} \tag{A21}$$

$$\frac{\partial\delta}{\partial n} = \frac{\left[\frac{Wd}{qS_t x_t} - \frac{di_t}{dn_t}\left(C_{L_{\alpha_t}}\right)_f - g\frac{l_t}{V^2}\frac{d\epsilon}{d\alpha}\left(C_{L_{\alpha_t}}\right)_f - \left(1 - \frac{d\epsilon}{d\alpha}\right)\left(C_{L_{\alpha_t}}\right)_f\frac{W}{a_F qS}\right]}{\left[\left(C_{L_{\alpha_t}}\right)_f \frac{d\alpha_t}{d\delta} + C_{m_\delta}\frac{\bar{c}_t}{x_t}\right]} \tag{A22}$$

and

$$\frac{\partial \delta}{\partial \ddot{\theta}} = \frac{\dfrac{I_{y_f}}{q S_t x_t} + 1.352\left(C_{l_{\alpha_t}}\right)_f \dfrac{di_t}{dn_t} + \left(1 - \dfrac{d\epsilon}{d\alpha}\right)\dfrac{\left(C_{L_{\alpha_t}}\right)_f I_{y_f}}{a_F x_t S q}}{\left[\left(C_{L_{\alpha_t}}\right)_f \dfrac{d\alpha_t}{d\delta} + C_{m_\delta} \dfrac{\bar{c}_t}{x_t}\right]} \tag{A23}$$

From equation (A21) the zero-lift pitching-moment coefficient $C_{m_0}$ may be derived as

$$C_{m_0} = -\frac{S_t x_t}{S \bar{c}} \left\{ \delta_0 \left[\left(C_{L_{\alpha_t}}\right)_f \frac{d\alpha_t}{d\delta} + C_{m_\delta} \frac{\bar{c}_t}{x_t}\right] - \left(C_{L_{\alpha_t}}\right)_f \left[3.00 + g \frac{l_t}{V^2} \frac{d\epsilon}{d\alpha} - \right. \right.$$

$$\left. \left. \left(1 - \frac{d\epsilon}{d\alpha}\right)\left(\alpha_{0_{adj}} + 2.75\right)\right] \right\} \tag{A24}$$

The aerodynamic-center location $d$ may be derived from equation (A22) as

$$d = \frac{l_t \left(C_{L_{\alpha_t}}\right)_f \left[\dfrac{\partial \delta}{\partial n} \dfrac{d\alpha_t}{d\delta} + \dfrac{di_t}{dn_t} + g \dfrac{l_t}{V^2} \dfrac{d\epsilon}{d\alpha} + \left(1 - \dfrac{d\epsilon}{d\alpha}\right)\dfrac{W}{a_F q S}\right] + \dfrac{\partial \delta}{\partial n} C_{m_\delta} \bar{c}_t}{\dfrac{W}{q S_t} - \left(C_{L_{\alpha_t}}\right)_f \left[\dfrac{\partial \delta}{\partial n} \dfrac{d\alpha_t}{d\delta} + \dfrac{di_t}{dn_t} + g \dfrac{l_t}{V^2} \dfrac{d\epsilon}{d\alpha} + \left(1 - \dfrac{d\epsilon}{d\alpha}\right)\dfrac{W}{a_F q S}\right]} \tag{A25}$$

and the effective moment of inertia $I_{y_f}$, from equation (A23) as

$$I_{y_f} = \frac{q S_t x_t}{1 + \left(1 - \dfrac{d\epsilon}{d\alpha}\right)\dfrac{S_t\left(C_{L_{\alpha_t}}\right)_f}{S a_F}} \left\{ \frac{\partial \delta}{\partial \ddot{\theta}} \left[\left(C_{l_{\alpha_t}}\right)_f \frac{d\alpha_t}{d\delta} + C_{m_\delta} \frac{\bar{c}_t}{x_t}\right] - 1.352\left(C_{l_{\alpha_t}}\right)_f \frac{di_t}{dn_t} \right\}$$

$$\tag{A26}$$

APPENDIX B


ANALYSIS OF BASIC DATA


As shown in appendix A the wing-fuselage aerodynamic-center position, zero-lift wing-fuselage pitching-moment coefficient, and effective moment of inertia may be determined from the coefficients of equations (A7) and (A19). The following sections give the least-squares procedures used for the determination of these coefficients and illustrative examples for both methods I and II.


Solutions by Use of Method I

For analysis of flight tail-load measurements for each maneuver, equations of the form of equation (A7) may be solved for the coefficients A, B, C, and D as follows:

$$\begin{Bmatrix} A \\ B \\ C \\ D \end{Bmatrix} = \left[ \begin{bmatrix} 1 & n & \ddot{\theta} & \dot{\theta}l_t/V \\ \cdot & \cdot & \cdot & \cdot \\ \cdot & \cdot & \cdot & \cdot \\ \cdot & \cdot & \cdot & \cdot \\ \cdot & \cdot & \cdot & \cdot \\ \cdot & \cdot & \cdot & \cdot \\ \cdot & \cdot & \cdot & \cdot \end{bmatrix}^T \begin{bmatrix} 1 & n & \ddot{\theta} & \dot{\theta}l_t/V \\ \cdot & \cdot & \cdot & \cdot \\ \cdot & \cdot & \cdot & \cdot \\ \cdot & \cdot & \cdot & \cdot \\ \cdot & \cdot & \cdot & \cdot \\ \cdot & \cdot & \cdot & \cdot \\ \cdot & \cdot & \cdot & \cdot \end{bmatrix} \right]^{-1} \begin{bmatrix} 1 & n & \ddot{\theta} & \dot{\theta}l_t/V \\ \cdot & \cdot & \cdot & \cdot \\ \cdot & \cdot & \cdot & \cdot \\ \cdot & \cdot & \cdot & \cdot \\ \cdot & \cdot & \cdot & \cdot \\ \cdot & \cdot & \cdot & \cdot \\ \cdot & \cdot & \cdot & \cdot \end{bmatrix}^T \begin{Bmatrix} L_{t_T} \\ \cdot \\ \cdot \\ \cdot \\ \cdot \\ \cdot \\ \cdot \end{Bmatrix} \qquad (B1)$$

In equation (B1) the individual rows of the rectangular matrix and the column matrix $L_{t_T}$ represent simultaneous measurements of the indicated parameters at each of various times in a given push-pull maneuver. Equation (B1) in the following equivalent form was used for the determination of the A, B, C, and D coefficients for each of the 68 maneuvers listed in table II:

$$\begin{Bmatrix} A \\ B \\ C \\ D \end{Bmatrix} = \begin{bmatrix} N & \sum n & \sum \ddot{\theta} & \sum \dot{\theta}l_t/V \\ \sum n & \sum n^2 & \sum \ddot{\theta}n & \sum \left(\dot{\theta}l_t/V\right)n \\ \sum \ddot{\theta} & \sum n\ddot{\theta} & \sum \ddot{\theta}^2 & \sum \left(\dot{\theta}l_t/V\right)\ddot{\theta} \\ \sum \dot{\theta}l_t/V & \sum n\left(\dot{\theta}l_t/V\right) & \sum \ddot{\theta}\left(\dot{\theta}l_t/V\right) & \sum \left(\dot{\theta}l_t/V\right)^2 \end{bmatrix}^{-1} \begin{Bmatrix} \sum L_{t_T} \\ \sum L_{t_T}n \\ \sum L_{t_T}\ddot{\theta} \\ \sum L_{t_T}\left(\dot{\theta}l_t/V\right) \end{Bmatrix} \quad (B2)$$

The determination of the A, B, C, and D coefficients for each maneuver by the use of equation (B2) requires time-history measurements of the following quantities:

n            normal load factor at center of gravity

$\ddot{\theta}$           pitching acceleration at center of gravity

$\dot{\theta}l_t/V$     tail angle of attack due to pitching velocity

$L_{t_T}$        aerodynamic tail load plus tail aerodynamic pitching moment

Figures 2 and 3 illustrate in time-history form the data used in the analysis of a typical maneuver (flight 12, run 27). The pitching acceleration $\ddot{\theta}$ has been corrected for instrument frequency-response characteristics.

The use of equation (B2) with the time-history data of figures 2 and 3 resulted in the following equation for tail load for this maneuver:

$$L_{t_T} = -1722 + 497n - 24150\ddot{\theta} + 82\dot{\theta}l_t/V \quad (B3)$$

The coefficient of $\dot{\theta}l_t/V$ was small in comparison with its standard error and the fit to the time history was not improved by the inclusion of this pitching-velocity parameter. Analysis of the other maneuvers also indicated that the parameter $\dot{\theta}l_t/V$ did not contribute significantly to the pitching-moment tail-load equation. Thus, for this and subsequent maneuvers the A, B, and C coefficients to be presented were obtained

by using equations of the form of equation (B2) with the $\dot{\theta}l_t/V$ term omitted. With the pitching-velocity term omitted, the equation determined as fitting the time history of $L_{t_T}$ for flight 12, run 27 became

$$L_{t_T} = -1702 + 392n - 24059\ddot{\theta} \tag{B4}$$

The calculated tail load $L_{t_T}$ (eq. (B4)) is compared in figure 3 with the measured time history from which it was derived. The fit is reasonably good and this sample maneuver is representative of the worst rather than the best correlation obtained.

The $A$, $B$, and $C$ coefficients obtained from the least-squares analysis of each of the 68 maneuvers are given in table III. Also listed in the table are the standard errors of fit and the standard errors of the individual coefficients.

### Solutions by Use of Method II

The elevator-angle equation (eq. (A19)) may be written in a form for least-squares solution of time-history data as follows:

$$
\begin{Bmatrix} \delta_0 \\[2mm] \dfrac{\partial\delta}{\partial n} \\[2mm] \dfrac{\partial\delta}{\partial\ddot{\theta}} \\[2mm] \dfrac{\partial\delta}{\partial\dot{\theta}l_t/V} \end{Bmatrix}
=
\begin{bmatrix}
N & \sum n & \sum \ddot{\theta} & \sum \dot{\theta}l_t/V \\[2mm]
\sum n & \sum n^2 & \sum \ddot{\theta}n & \sum (\dot{\theta}l_t/V)n \\[2mm]
\sum \ddot{\theta} & \sum n\ddot{\theta} & \sum \ddot{\theta}^2 & \sum (\dot{\theta}l_t/V)\ddot{\theta} \\[2mm]
\sum \dot{\theta}l_t/V & \sum n(\dot{\theta}l_t/V) & \sum \ddot{\theta}(\dot{\theta}l_t/V) & \sum (\dot{\theta}l_t/V)^2
\end{bmatrix}^{-1}
\begin{Bmatrix} \sum \delta \\[2mm] \sum \delta n \\[2mm] \sum \delta\ddot{\theta} \\[2mm] \sum \delta(\dot{\theta}l_t/V) \end{Bmatrix}
\tag{B5}
$$

In figure 4 the elevator angle is shown in time-history form for the example maneuver (flight 12, run 27). When the elevator-angle data are used in addition to the data shown in figure 3, the following equation is obtained by solution of equation (B5):

$$\delta = 4.548 + 3.534\frac{\dot{\theta}l_t}{V} - 6.620n - 21.563\ddot{\theta} \tag{B6}$$

In this case the term $\dot{\theta} l_t/V$ is an important parameter and is retained for all solutions. A time history of the elevator angles computed by use of equation (B6) is shown in figure 4. The agreement is reasonably good but again the example maneuver is not as good a fit as was obtained with the majority of the maneuvers analyzed.

The elevator-angle coefficients of equation (B5) for all 68 maneuvers are listed in table IV along with their standard errors and errors of fit.

REFERENCES

1. Mayo, Alton P., and Ward, John F.: Experimental Influence Coefficients
   for the Deflection of the Wing of a Full-Scale, Swept-Wing Bomber.
   NACA RM L53L23, 1954.

2. Mayo, Alton P., and Ward, John F.: Flight Investigation and Analysis
   of the Wing Deformations of a Swept-Wing Bomber During Push-Pull
   Maneuvers. NACA RM L54K24a, 1955.

3. Aiken, William S., Jr., and Fisher, Raymond A.: Horizontal-Tail
   Parameters As Determined From Flight-Test Tail Loads on a Flexible
   Swept-Wing Jet Bomber. NACA RM L56J02, 1957.

4. Aiken, William S., Jr., and Fisher, Raymond A.: Lift-Curve Slopes
   Determined in Flight on a Flexible Swept-Wing Jet Bomber. NACA
   RM L56E21a, 1956.

5. Gainer, Patrick A., and Harper, Paul W.: Analysis of Wing Loads
   Measured on a Flexible Swept-Wing Jet Bomber During Push-Pull
   Maneuvers. NACA RM L57E28, 1957.

6. Skopinski, T. H., Aiken, William S., Jr., and Huston, Wilber B.:
   Calibration of Strain-Gage Installations in Aircraft Structures
   for the Measurement of Flight Loads. NACA Rep. 1178, 1954.
   (Supersedes NACA TN 2993.)

7. Budish, Nathan N.: Longitudinal Stability at High Airspeeds. Doc.
   No. D-8603-0 (Contract No. W33-038 ac-22413), Boeing Airplane Co.,
   Feb. 29, 1952.

8. Brown, R. B., Holtby, K. F., and Martin, H. C.: A Superposition
   Method for Calculating the Aeroelastic Behavior of Swept Wings.
   Jour. Aero. Sci., vol. 18, no. 8, Aug. 1951, pp. 531-542.

9. Cole, Henry A., Jr., and Bennion, Frances L.: Measurement of the
   Longitudinal Moment of Inertia of a Flexible Airplane. NACA
   TN 3870, 1956. (Supersedes NACA RM A55J21.)

10. Gray, W. L., and Schenk, K. M.: A Method for Calculating the Sub-
    sonic Steady-State Loading on an Airplane With a Wing of Arbitrary
    Plan Form and Stiffness. NACA TN 3030, 1953.

11. Mayo, Alton P.: Flight Investigation and Theoretical Calculations
    of the Fuselage Deformations of a Swept-Wing Bomber During Push-
    Pull Maneuvers. NACA RM L56L05, 1957.

TABLE I.- AIRPLANE CHARACTERISTICS AND DIMENSIONS

Horizontal tail:
    Total area, sq ft . . . . . . . . . . . . . . . . . . . . . . . . . .    268
    Span, ft . . . . . . . . . . . . . . . . . . . . . . . . . . . . . .    33
    Root chord, ft . . . . . . . . . . . . . . . . . . . . . . . . . . .    11.42
    Mean aerodynamic chord, ft . . . . . . . . . . . . . . . . . . . .    8.58
    Distance from horizontal-tail 25 percent M.A.C. to wing
      25 percent M.A.C., ft . . . . . . . . . . . . . . . . . . . . . .    46.52
    Incidence angle, deg . . . . . . . . . . . . . . . . . . . . . . .    -0.25
    Sweepback (25-percent-chord line), deg . . . . . . . . . . .    32.9
    Aspect ratio . . . . . . . . . . . . . . . . . . . . . . . . . . .    4.06
    Taper ratio . . . . . . . . . . . . . . . . . . . . . . . . . . . .    0.423
    Airfoil section . . . . . . . . . . . . . . . . . . . . . . . . . . BAC 100
    Strain-gage reference station (percent semispan) . . . . . .    5.3

Wing:
    Total area, sq ft . . . . . . . . . . . . . . . . . . . . . . . .    1,428
    Span, ft . . . . . . . . . . . . . . . . . . . . . . . . . . . . . .    116
    Mean aerodynamic chord, in. . . . . . . . . . . . . . . . . . . .    155.9
    Aspect ratio . . . . . . . . . . . . . . . . . . . . . . . . . . .    9.42
    Taper ratio . . . . . . . . . . . . . . . . . . . . . . . . . . . .    0.420
    Incidence angle, deg . . . . . . . . . . . . . . . . . . . . . . .    2.75
    Sweepback (25-percent-chord line), deg . . . . . . . . . . .    35
    Airfoil section . . . . . . . . . . . . . . . . . . . . . . . . . . BAC 145

TABLE II.- SUMMARY OF FLIGHT CONDITIONS

| Flight | Run | $\bar{M}$ | $\bar{q}$, lb/sq ft | Pressure altitude, ft | W, lb | Center-of-gravity location, percent M.A.C. |
|---|---|---|---|---|---|---|
| 2 | 27 | 0.636 ± 0.002 | 137 ± 2 | 35,200 | 112,600 | 22.2 |
|  | 28 | 0.735 ± 0.001 | 184 ± 1 | 34,900 | 112,300 | 21.8 |
|  | 29 | 0.796 ± 0.004 | 216 ± 2 | 34,800 | 112,200 | 21.7 |
| 3 | 11 | 0.750 ± 0.001 | 196 ± 1 | 34,600 | 120,300 | 14.1 |
|  | 12 | 0.728 ± 0.007 | 188 ± 5 | 34,100 | 120,100 | 14.2 |
|  | 13 | 0.689 ± 0.006 | 167 ± 3 | 34,400 | 119,900 | 14.3 |
|  | 14 | 0.631 ± 0.002 | 140 ± 1 | 34,600 | 119,000 | 14.5 |
| 4 | 19 | 0.699 ± 0.002 | 264 ± 3 | 25,000 | 108,900 | 21.2 |
|  | 20 | 0.591 ± 0.001 | 190 ± 1 | 25,000 | 108,700 | 21.5 |
|  | 21 | 0.486 ± 0.003 | 128 ± 1 | 25,300 | 108,400 | 22.1 |
| 6 | 11 | 0.789 ± 0.001 | 264 ± 3 | 30,800 | 108,800 | 13.3 |
|  | 12 | 0.790 ± 0.001 | 268 ± 1 | 30,500 | 108,700 | 13.3 |
|  | 13 | 0.741 ± 0.001 | 244 ± 1 | 29,800 | 108,400 | 13.3 |
|  | 14 | 0.690 ± 0.001 | 215 ± 1 | 29,400 | 108,200 | 13.6 |
|  | 15 | 0.643 ± 0.003 | 187 ± 2 | 29,400 | 107,600 | 13.6 |
| 8 | 4 | 0.544 ± 0.008 | 163 ± 4 | 24,900 | 124,800 | 23.6 |
|  | 5 | 0.648 ± 0.004 | 233 ± 3 | 24,900 | 124,500 | 23.3 |
|  | 6 | 0.758 ± 0.002 | 314 ± 4 | 25,100 | 124,000 | 23.3 |
| 9 | 1 | 0.598 ± 0.003 | 125 ± 1 | 34,800 | 126,700 | 24.1 |
|  | 2 | 0.647 ± 0.004 | 147 ± 2 | 34,900 | 126,200 | 23.7 |
|  | 3 | 0.681 ± 0.001 | 161 ± 1 | 35,200 | 126,100 | 23.7 |
|  | 4 | 0.731 ± 0.005 | 185 ± 1 | 35,200 | 125,700 | 23.6 |
|  | 5 | 0.779 ± 0.002 | 214 ± 1 | 34,900 | 125,400 | 23.4 |
|  | 6 | 0.795 ± 0.001 | 216 ± 1 | 35,500 | 125,200 | 23.7 |
|  | 7 | 0.810 ± 0 | 225 ± 1 | 35,300 | 124,900 | 23.9 |
| 10 | 3 | 0.598 ± 0.003 | 159 ± 2 | 29,800 | 127,200 | 23.7 |
|  | 4 | 0.647 ± 0.001 | 185 ± 0 | 29,900 | 126,500 | 23.1 |
|  | 5 | 0.681 ± 0.001 | 200 ± 1 | 30,500 | 126,300 | 23.1 |
|  | 6 | 0.726 ± 0.001 | 230 ± 1 | 30,200 | 126,100 | 23.0 |
|  | 7 | 0.763 ± 0 | 254 ± 0 | 30,200 | 125,400 | 23.2 |
|  | 8 | 0.789 ± 0.001 | 260 ± 1 | 31,100 | 125,200 | 23.4 |
|  | 9 | 0.812 ± 0.001 | 274 ± 1 | 31,300 | 124,900 | 23.5 |
| 11 | 11 | 0.495 ± 0.003 | 138 ± 1 | 24,400 | 109,200 | 23.0 |
|  | 12 | 0.542 ± 0.003 | 164 ± 1 | 24,600 | 108,900 | 22.5 |
|  | 13 | 0.597 ± 0.001 | 194 ± 1 | 25,100 | 108,500 | 22.3 |
|  | 14 | 0.636 ± 0 | 222 ± 0 | 25,000 | 108,500 | 22.2 |
|  | 15 | 0.681 ± 0 | 247 ± 0 | 25,700 | 108,400 | 22.4 |
|  | 16 | 0.702 ± 0.001 | 266 ± 1 | 25,400 | 107,800 | 21.9 |
|  | 17 | 0.734 ± 0 | 291 ± 1 | 25,300 | 107,500 | 21.9 |
|  | 24 | 0.427 ± 0.001 | 126 ± 1 | 19,700 | 103,700 | 23.8 |
| 12 | 6 | 0.584 ± 0.001 | 127 ± 1 | 33,700 | 120,400 | 15.9 |
|  | 7 | 0.642 ± 0.001 | 147 ± 1 | 34,400 | 120,300 | 15.7 |
|  | 8 | 0.679 ± 0.001 | 162 ± 0 | 34,900 | 119,900 | 15.5 |
|  | 9 | 0.721 ± 0.001 | 178 ± 1 | 35,300 | 119,600 | 15.2 |
|  | 10 | 0.773 ± 0.001 | 202 ± 1 | 35,400 | 119,100 | 15.2 |
|  | 11 | 0.790 ± 0 | 215 ± 0 | 35,200 | 118,800 | 14.9 |
|  | 12 | 0.812 ± 0 | 228 ± 0 | 35,200 | 118,700 | 14.7 |
|  | 17 | 0.483 ± 0.001 | 130 ± 1 | 24,600 | 116,600 | 15.3 |
|  | 18 | 0.532 ± 0 | 157 ± 0 | 24,700 | 116,500 | 14.8 |
|  | 19 | 0.600 ± 0.001 | 198 ± 1 | 24,900 | 116,400 | 14.3 |
|  | 20 | 0.637 ± 0 | 223 ± 0 | 25,000 | 116,300 | 14.3 |
|  | 21 | 0.682 ± 0.001 | 255 ± 1 | 25,000 | 116,100 | 14.5 |
|  | 22 | 0.694 ± 0.001 | 262 ± 0 | 25,200 | 115,800 | 14.3 |
|  | 23 | 0.735 ± 0.001 | 298 ± 1 | 24,900 | 115,400 | 14.4 |
|  | 24 | 0.642 ± 0.002 | 279 ± 3 | 20,000 | 111,100 | 21.7 |
|  | 25 | 0.595 ± 0.002 | 242 ± 1 | 19,800 | 111,100 | 21.8 |
|  | 26 | 0.543 ± 0 | 202 ± 1 | 19,700 | 110,600 | 22.2 |
|  | 27 | 0.482 ± 0.002 | 159 ± 1 | 19,700 | 110,300 | 22.9 |
|  | 28 | 0.427 ± 0.001 | 126 ± 1 | 19,600 | 110,200 | 23.1 |
| 16 | 1 | 0.642 ± 0.001 | 282 ± 1 | 19,900 | 117,100 | 14.8 |
|  | 2 | 0.599 ± 0.002 | 246 ± 2 | 19,800 | 116,800 | 14.7 |
|  | 3 | 0.542 ± 0.002 | 200 ± 2 | 20,000 | 116,600 | 14.2 |
|  | 4 | 0.482 ± 0.002 | 160 ± 1 | 19,800 | 116,000 | 14.9 |
|  | 5 | 0.428 ± 0.003 | 127 ± 2 | 19,500 | 115,500 | 15.2 |
|  | 6 | 0.433 ± 0.002 | 131 ± 2 | 19,300 | 115,100 | 14.9 |
| 17 | 5 | 0.808 ± 0.001 | 364 ± 1 | 24,600 | 116,400 | 14.1 |
|  | 6 | 0.762 ± 0 | 326 ± 0 | 24,500 | 116,200 | 14.2 |
|  | 7 | 0.725 ± 0 | 295 ± 0 | 24,500 | 115,600 | 14.1 |

TABLE III.- MEASURED TAIL-LOAD COEFFICIENTS OBTAINED BY USE OF EQUATION (B2)

| Flight | Run | A | $\epsilon_A$ | B | $\epsilon_B$ | C | $\epsilon_C$ | Standard error |
|---|---|---|---|---|---|---|---|---|
| 2 | 27 | -1,264 | ±184 | 279 | ±180 | -30,725 | ±980 | 104 |
|   | 28 | -4,207 | ±288 | 920 | ±180 | -28,944 | ±861 | 122 |
|   | 29 | -6,553 | ±312 | 776 | ±121 | -29,533 | ±811 | 78 |
| 3 | 11 | -2,143 | ±207 | -1,260 | ±149 | -29,823 | ±849 | 95 |
|   | 12 | -1,627 | ±99 | -1,446 | ±84 | -31,656 | ±611 | 123 |
|   | 13 | -799 | ±93 | -1,420 | ±76 | -30,567 | ±722 | 89 |
|   | 14 | 385 | ±81 | -1,575 | ±106 | -31,408 | ±578 | 69 |
| 4 | 19 | -6,451 | ±191 | 1,108 | ±77 | -24,466 | ±424 | 69 |
|   | 20 | -4,272 | ±206 | 691 | ±133 | -24,964 | ±500 | 95 |
|   | 21 | -1,181 | ±185 | 91 | ±202 | -26,844 | ±625 | 94 |
| 6 | 11 | -3,782 | ±123 | -1,558 | ±101 | -26,492 | ±626 | 85 |
|   | 12 | -4,543 | ±214 | -1,016 | ±92 | -22,263 | ±485 | 76 |
|   | 13 | -3,352 | ±357 | -1,305 | ±211 | -23,929 | ±755 | 146 |
|   | 14 | -2,062 | ±343 | -1,610 | ±229 | -26,189 | ±984 | 141 |
|   | 15 | -1,494 | ±242 | -1,286 | ±182 | -24,484 | ±793 | 105 |
| 8 | 4 | 8,575 | ±292 | 1,302 | ±111 | -27,745 | ±743 | 69 |
|   | 5 | 6,254 | ±132 | 1,805 | ±99 | -27,986 | ±460 | 101 |
|   | 6 | 2,096 | ±50 | 2,238 | ±88 | -26,878 | ±411 | 89 |
| 9 | 1 | 14,921 | ±352 | 1,259 | ±144 | -31,453 | ±533 | 91 |
|   | 2 | 12,385 | ±597 | 1,553 | ±121 | -30,431 | ±1,012 | 110 |
|   | 3 | 10,074 | ±338 | 1,526 | ±114 | -30,379 | ±670 | 73 |
|   | 4 | 7,494 | ±217 | 1,948 | ±144 | -28,856 | ±493 | 98 |
|   | 5 | 3,910 | ±125 | 2,073 | ±79 | -27,788 | ±461 | 89 |
|   | 6 | 2,723 | ±190 | 1,418 | ±211 | -30,925 | ±1,204 | 108 |
|   | 7 | 1,815 | ±187 | 1,000 | ±205 | -30,484 | ±1,321 | 91 |
| 10 | 3 | 11,828 | ±326 | 988 | ±218 | -30,098 | ±727 | 153 |
|   | 4 | 9,410 | ±281 | 1,091 | ±285 | -32,209 | ±875 | 203 |
|   | 5 | 7,705 | ±200 | 1,124 | ±262 | -29,850 | ±686 | 128 |
|   | 6 | 3,218 | ±84 | 1,775 | ±136 | -28,107 | ±416 | 98 |
|   | 7 | 1,170 | ±106 | 1,554 | ±168 | -29,071 | ±536 | 87 |
|   | 8 | -673 | ±296 | 1,807 | ±381 | -27,558 | ±960 | 182 |
|   | 9 | -1,116 | ±126 | 1,379 | ±130 | -28,669 | ±487 | 106 |
| 11 | 11 | 562 | ±386 | 164 | ±507 | -26,600 | ±953 | 295 |
|   | 12 | -532 | ±155 | 417 | ±185 | -26,567 | ±553 | 146 |
|   | 13 | -1,650 | ±104 | 669 | ±104 | -26,062 | ±406 | 89 |
|   | 14 | -3,797 | ±209 | 1,057 | ±156 | -24,022 | ±521 | 161 |
|   | 15 | -4,566 | ±263 | 1,009 | ±171 | -24,700 | ±624 | 210 |
|   | 16 | -5,821 | ±221 | 1,257 | ±142 | -23,845 | ±406 | 148 |
|   | 17 | -7,315 | ±267 | 1,382 | ±143 | -22,164 | ±416 | 124 |
|   | 24 | -257 | ±286 | 501 | ±216 | -26,232 | ±1,263 | 108 |
| 12 | 6 | 6,965 | ±216 | -716 | ±320 | -26,798 | ±598 | 180 |
|   | 7 | 5,332 | ±259 | -378 | ±363 | -25,781 | ±683 | 284 |
|   | 8 | 4,988 | ±473 | -1,873 | ±658 | -27,161 | ±943 | 280 |
|   | 9 | 2,387 | ±203 | -592 | ±297 | -25,096 | ±607 | 279 |
|   | 10 | -286 | ±697 | -715 | ±874 | -23,892 | ±1,313 | 480 |
|   | 11 | -1,028 | ±656 | -1,022 | ±750 | -24,865 | ±1,268 | 366 |
|   | 12 | -2,766 | ±679 | -1,283 | ±456 | -24,518 | ±838 | 169 |
|   | 17 | -4,802 | ±512 | -1,450 | ±395 | -26,425 | ±642 | 222 |
|   | 18 | -5,436 | ±338 | -1,588 | ±244 | -26,273 | ±467 | 152 |
|   | 19 | -7,554 | ±309 | -604 | ±165 | -24,821 | ±377 | 191 |
|   | 20 | -8,451 | ±402 | -650 | ±217 | -24,479 | ±474 | 186 |
|   | 21 | -9,518 | ±432 | -651 | ±226 | -24,257 | ±491 | 155 |
|   | 22 | -9,504 | ±510 | -538 | ±256 | -23,682 | ±581 | 211 |
|   | 23 | -10,676 | ±321 | -263 | ±135 | -23,659 | ±346 | 130 |
|   | 24 | -7,060 | ±305 | 1,338 | ±184 | -22,970 | ±440 | 158 |
|   | 25 | -5,765 | ±259 | 1,027 | ±173 | -23,259 | ±380 | 163 |
|   | 26 | -3,765 | ±166 | 842 | ±128 | -24,437 | ±354 | 115 |
|   | 27 | -1,702 | ±363 | 392 | ±358 | -24,059 | ±637 | 267 |
|   | 28 | -880 | ±461 | 401 | ±478 | -24,726 | ±821 | 289 |
| 16 | 1 | 2,268 | ±80 | -824 | ±114 | -26,414 | ±347 | 90 |
|   | 2 | 2,367 | ±138 | -870 | ±158 | -25,959 | ±454 | 135 |
|   | 3 | 3,050 | ±141 | -1,263 | ±169 | -27,119 | ±557 | 117 |
|   | 4 | 3,202 | ±134 | -1,467 | ±161 | -27,302 | ±496 | 90 |
|   | 5 | 3,588 | ±97 | -1,973 | ±113 | -28,371 | ±419 | 71 |
|   | 6 | 2,789 | ±69 | -1,677 | ±80 | -27,929 | ±242 | 70 |
| 17 | 5 | -5,376 | ±246 | -166 | ±126 | -22,942 | ±457 | 135 |
|   | 6 | -3,392 | ±272 | -384 | ±188 | -24,246 | ±561 | 221 |
|   | 7 | -1,383 | ±436 | -1,260 | ±393 | -26,152 | ±932 | 225 |

TABLE IV.- MEASURED ELEVATOR-ANGLE COEFFICIENTS OBTAINED BY USE OF EQUATION (B5)

| Flight | Run | $\delta_0$ | $\epsilon_{\delta_0}$ | $\dfrac{\partial \delta}{\partial \frac{\dot{\theta}_t}{V}}$ | $\epsilon \partial \delta/\partial(\dot{\theta}_t/V)$ | $\dfrac{\partial \delta}{\partial n}$ | $\epsilon_{\partial \delta/\partial n}$ | $\dfrac{\partial \delta}{\partial \ddot{\theta}}$ | $\epsilon_{\partial \delta/\partial \ddot{\theta}}$ | Standard error |
|---|---|---|---|---|---|---|---|---|---|---|
| 2 | 27 | 3.502 | ±0.125 | 4.648 | ±0.163 | -6.514 | ±0.145 | -27.369 | ±0.244 | 0.077 |
|   | 28 | 3.456 | ±.145 | 4.606 | ±.276 | -4.467 | ±.150 | -19.595 | ±.240 | .099 |
|   | 29 | 3.114 | ±.078 | 5.282 | ±.233 | -3.357 | ±.085 | -15.547 | ±.183 | .048 |
| 3 | 11 | 3.105 | ±.157 | 4.573 | ±.244 | -6.123 | ±.186 | -19.835 | ±.270 | .068 |
|   | 12 | 3.408 | ±.124 | 3.500 | ±.371 | -6.680 | ±.144 | -22.237 | ±.157 | .137 |
|   | 13 | 3.397 | ±.127 | 4.013 | ±.289 | -7.672 | ±.132 | -23.061 | ±.324 | .111 |
|   | 14 | 3.895 | ±.111 | 3.212 | ±.159 | -9.815 | ±.146 | -31.507 | ±.232 | .072 |
| 4 | 19 | 4.130 | ±.061 | 4.031 | ±.173 | -3.995 | ±.065 | -14.042 | ±.220 | .055 |
|   | 20 | 4.074 | ±.151 | 3.599 | ±.190 | -5.763 | ±.162 | -19.839 | ±.200 | .106 |
|   | 21 | 4.055 | ±.273 | 3.251 | ±.185 | -8.062 | ±.339 | -27.583 | ±.318 | .112 |
| 6 | 11 | 3.219 | ±.067 | 4.848 | ±.225 | -4.303 | ±.074 | -12.627 | ±.121 | .047 |
|   | 12 | 3.225 | ±.098 | 4.881 | ±.216 | -4.279 | ±.099 | -12.335 | ±.132 | .060 |
|   | 13 | 3.447 | ±.155 | 4.101 | ±.191 | -4.768 | ±.150 | -13.523 | ±.145 | .083 |
|   | 14 | 3.827 | ±.190 | 4.080 | ±.243 | -5.876 | ±.192 | -17.037 | ±.212 | .089 |
|   | 15 | 3.484 | ±.254 | 3.862 | ±.252 | -6.426 | ±.254 | -18.269 | ±.286 | .106 |
| 8 | 4 | 3.553 | ±.108 | 3.321 | ±.186 | -6.334 | ±.119 | -22.399 | ±.270 | .063 |
|   | 5 | 4.232 | ±.063 | 3.829 | ±.135 | -4.597 | ±.063 | -17.372 | ±.110 | .070 |
|   | 6 | 3.945 | ±.035 | 4.700 | ±.102 | -3.163 | ±.037 | -12.170 | ±.073 | .045 |
| 9 | 1 | 2.641 | ±.177 | 3.936 | ±.164 | -7.225 | ±.224 | -30.945 | ±.306 | .108 |
|   | 2 | 3.491 | ±.249 | 3.702 | ±.204 | -6.594 | ±.308 | -25.691 | ±.390 | .082 |
|   | 3 | 3.564 | ±.094 | 4.362 | ±.156 | -5.625 | ±.111 | -21.500 | ±.271 | .066 |
|   | 4 | 5.074 | ±.192 | 3.724 | ±.284 | -4.570 | ±.232 | -20.438 | ±.328 | .088 |
|   | 5 | 2.960 | ±.089 | 4.387 | ±.170 | -3.504 | ±.076 | -17.589 | ±.166 | .101 |
|   | 6 | 3.157 | ±.147 | 4.682 | ±.309 | -3.398 | ±.178 | -17.349 | ±.324 | .080 |
|   | 7 | 3.335 | ±.245 | 5.067 | ±.465 | -3.630 | ±.311 | -17.199 | ±.535 | .109 |
| 10 | 3 | 3.494 | ±.142 | 3.900 | ±.104 | -6.650 | ±.145 | -26.204 | ±.164 | .105 |
|   | 4 | 4.445 | ±.189 | 3.851 | ±.168 | -5.994 | ±.213 | -24.175 | ±.220 | .143 |
|   | 5 | 4.088 | ±.198 | 4.333 | ±.178 | -5.034 | ±.222 | -20.248 | ±.196 | .091 |
|   | 6 | 3.728 | ±.098 | 4.556 | ±.131 | -4.357 | ±.105 | -17.556 | ±.117 | .081 |
|   | 7 | 3.885 | ±.107 | 4.506 | ±.159 | -3.788 | ±.122 | -15.881 | ±.133 | .051 |
|   | 8 | 3.889 | ±.170 | 4.925 | ±.249 | -3.447 | ±.193 | -14.758 | ±.175 | .084 |
|   | 9 | 3.328 | ±.079 | 5.353 | ±.185 | -3.085 | ±.080 | -13.770 | ±.104 | .068 |
| 11 | 11 | 4.312 | ±.504 | 3.609 | ±.274 | -6.959 | ±.617 | -25.417 | ±.385 | .268 |
|   | 12 | 4.500 | ±.175 | 3.550 | ±.150 | -6.032 | ±.210 | -21.805 | ±.195 | .112 |
|   | 13 | 4.281 | ±.113 | 3.581 | ±.142 | -5.244 | ±.135 | -18.964 | ±.163 | .072 |
|   | 14 | 4.411 | ±.110 | 3.883 | ±.159 | -4.602 | ±.122 | -16.518 | ±.137 | .102 |
|   | 15 | 4.348 | ±.095 | 4.251 | ±.161 | -4.067 | ±.106 | -15.095 | ±.121 | .107 |
|   | 16 | 4.359 | ±.119 | 4.128 | ±.180 | -3.777 | ±.137 | -13.936 | ±.128 | .106 |
|   | 17 | 4.162 | ±.088 | 4.199 | ±.147 | -3.525 | ±.105 | -12.152 | ±.103 | .082 |
|   | 24 | 3.805 | ±.357 | 3.287 | ±.560 | -7.096 | ±.321 | -28.281 | ±.416 | .103 |
| 12 | 6 | 1.912 | ±.488 | 4.254 | ±.256 | -8.187 | ±.579 | -26.922 | ±.339 | .210 |
|   | 7 | 2.396 | ±.396 | 4.254 | ±.237 | -7.097 | ±.448 | -23.442 | ±.249 | .226 |
|   | 8 | 2.370 | ±.428 | 4.902 | ±.197 | -5.917 | ±.507 | -20.762 | ±.278 | .156 |
|   | 9 | 4.031 | ±.201 | 4.124 | ±.191 | -6.808 | ±.259 | -19.980 | ±.154 | .209 |
|   | 10 | 3.058 | ±.540 | 5.052 | ±.468 | -4.926 | ±.670 | -15.822 | ±.355 | .346 |
|   | 11 | 3.744 | ±.493 | 4.701 | ±.541 | -5.403 | ±.594 | -16.056 | ±.327 | .256 |
|   | 12 | 3.726 | ±.324 | 5.008 | ±.272 | -4.991 | ±.404 | -14.843 | ±.239 | .132 |
|   | 17 | 3.622 | ±.651 | 3.611 | ±.219 | -9.588 | ±.694 | -28.126 | ±.316 | .283 |
|   | 18 | 4.059 | ±.328 | 3.582 | ±.165 | -8.592 | ±.375 | -24.189 | ±.199 | .151 |
|   | 19 | 4.503 | ±.144 | 3.663 | ±.102 | -7.185 | ±.134 | -20.376 | ±.090 | .141 |
|   | 20 | 4.594 | ±.141 | 3.856 | ±.094 | -6.500 | ±.149 | -17.992 | ±.095 | .114 |
|   | 21 | 4.632 | ±.167 | 4.053 | ±.143 | -5.772 | ±.194 | -15.667 | ±.123 | .097 |
|   | 22 | 4.212 | ±.186 | 4.265 | ±.178 | -5.282 | ±.214 | -14.488 | ±.142 | .137 |
|   | 23 | 4.252 | ±.103 | 4.915 | ±.112 | -4.686 | ±.107 | -13.443 | ±.082 | .094 |
|   | 24 | 4.438 | ±.094 | 4.038 | ±.104 | -3.892 | ±.100 | -13.193 | ±.082 | .091 |
|   | 25 | 4.378 | ±.109 | 3.936 | ±.096 | -4.651 | ±.110 | -15.534 | ±.079 | .104 |
|   | 26 | 4.072 | ±.104 | 3.683 | ±.100 | -5.202 | ±.110 | -17.859 | ±.098 | .093 |
|   | 27 | 4.548 | ±.239 | 3.534 | ±.130 | -6.620 | ±.258 | -21.563 | ±.144 | .180 |
|   | 28 | 3.985 | ±.468 | 3.393 | ±.191 | -7.772 | ±.500 | -26.485 | ±.267 | .278 |
| 16 | 1 | 4.573 | ±.078 | 3.805 | ±.087 | -5.475 | ±.081 | -15.842 | ±.084 | .062 |
|   | 2 | 3.955 | ±.111 | 3.913 | ±.106 | -5.885 | ±.114 | -16.838 | ±.092 | .081 |
|   | 3 | 4.196 | ±.159 | 3.561 | ±.121 | -7.165 | ±.170 | -20.882 | ±.149 | .083 |
|   | 4 | 4.164 | ±.271 | 3.590 | ±.163 | -8.688 | ±.293 | -25.164 | ±.241 | .104 |
|   | 5 | 4.023 | ±.151 | 3.388 | ±.087 | -10.629 | ±.165 | -30.696 | ±.158 | .072 |
|   | 6 | 3.181 | ±.159 | 3.659 | ±.085 | -9.254 | ±.173 | -28.111 | ±.137 | .107 |
| 17 | 5 | 3.937 | ±.089 | 5.758 | ±.155 | -3.569 | ±.094 | -10.948 | ±.100 | .086 |
|   | 6 | 3.777 | ±.139 | 4.699 | ±.183 | -4.075 | ±.144 | -12.114 | ±.125 | .142 |
|   | 7 | 4.094 | ±.261 | 5.042 | ±.231 | -4.721 | ±.292 | -13.946 | ±.191 | .115 |

TABLE V.- AERODYNAMIC-CENTER POSITION

| Group $M$ | Group $(X_{ac})_r$ | Flight | Run | $M$ | $q_R$ | $(X_{ac})_{flex}$ (method I) | $(X_{ac})_{flex}$ (method II) | $\Delta X_{ac}$ | $(X_{ac})_r$ (method I) | $(X_{ac})_r$ (method II) |
|---|---|---|---|---|---|---|---|---|---|---|
| 0.429 | 25.71 ± 0.52 | 11 | 24 | 0.427 | 11.4 | 22.1 ± 0.7 | 20.6 ± 0.9 | 3.5 | 25.6 | 24.1 |
| | | 12 | 28 | .427 | 11.4 | 21.8 ± 1.5 | 20.7 ± 1.4 | 3.5 | 25.3 | 24.2 |
| | | 16 | 5 | .428 | 11.5 | 21.3 ± 0.3 | 19.8 ± 0.4 | 3.5 | 24.8 | 23.3 |
| | | 16 | 6 | .433 | 11.9 | 20.1 ± 0.3 | 16.4 ± 0.5 | 3.6 | 23.7 | 20.0 |
| .486 | 24.45 ± 0.35 | 12 | 27 | .482 | 14.7 | 21.6 ± 1.2 | 20.8 ± 0.9 | 4.4 | 26.0 | 25.2 |
| | | 16 | 4 | .482 | 14.8 | 19.4 ± 0.5 | 18.7 ± 0.9 | 4.4 | 23.8 | 23.1 |
| | | 12 | 17 | .483 | 12.0 | 19.7 ± 1.2 | 18.0 ± 1.9 | 3.6 | 23.3 | 21.6 |
| | | 4 | 21 | .486 | 11.9 | 21.8 ± 0.7 | 21.9 ± 1.0 | 3.6 | 25.4 | 25.5 |
| | | 11 | 11 | .495 | 12.8 | 22.5 ± 1.6 | 20.3 ± 1.9 | 3.9 | 26.4 | 24.2 |
| .541 | 24.10 ± 0.27 | 12 | 18 | .532 | 14.8 | 19.7 ± 0.8 | 18.6 ± 1.2 | 4.4 | 24.1 | 23.2 |
| | | 11 | 12 | .542 | 15.6 | 21.1 ± 0.6 | 19.7 ± 0.7 | 4.6 | 25.7 | 24.3 |
| | | 16 | 3 | .542 | 19.0 | 18.1 ± 0.5 | 16.8 ± 0.6 | 5.5 | 23.6 | 22.3 |
| | | 12 | 26 | .543 | 19.2 | 19.5 ± 0.4 | 18.4 ± 0.4 | 5.5 | 25.0 | 23.9 |
| | | 8 | 4 | .544 | 15.5 | 19.9 ± 0.3 | 18.5 ± 0.4 | 4.6 | 24.5 | 23.1 |
| .595 | 24.33 ± 0.31 | 12 | 6 | .584 | 12.3 | 18.0 ± 1.0 | 14.8 ± 1.6 | 3.7 | 21.7 | 18.5 |
| | | 4 | 20 | .591 | 18.5 | 19.2 ± 0.4 | 20.6 ± 0.6 | 5.4 | 24.6 | 26.0 |
| | | 12 | 25 | .595 | 23.6 | 18.5 ± 0.6 | 18.2 ± 0.5 | 6.7 | 25.2 | 24.9 |
| | | 11 | 13 | .597 | 18.9 | 20.1 ± 0.3 | 19.2 ± 0.5 | 5.5 | 25.6 | 24.7 |
| | | 10 | 3 | .598 | 15.5 | 20.9 ± 0.6 | 19.8 ± 0.4 | 4.6 | 25.5 | 24.4 |
| | | 9 | 1 | .598 | 12.2 | 20.6 ± 0.4 | 18.8 ± 0.6 | 3.7 | 24.3 | 22.5 |
| | | 16 | 2 | .599 | 24.0 | 17.4 ± 0.5 | 15.6 ± 0.5 | 6.8 | 24.2 | 22.4 |
| | | 12 | 19 | .600 | 19.3 | 16.2 ± 0.5 | 18.3 ± 0.5 | 5.6 | 21.8 | 23.9 |
| .635 | 24.23 ± 0.33 | 3 | 14 | .631 | 13.9 | 19.2 ± 0.3 | 21.3 ± 0.4 | 4.2 | 23.4 | 25.5 |
| | | 2 | 27 | .636 | 13.6 | 21.3 ± 0.6 | 19.5 ± 0.4 | 4.1 | 25.4 | 23.6 |
| | | 11 | 14 | .637 | 22.1 | 18.7 ± 0.5 | 18.5 ± 0.5 | 6.3 | 25.0 | 24.8 |
| | | 12 | 20 | .637 | 22.2 | 16.3 ± 0.7 | 17.9 ± 0.6 | 6.3 | 22.6 | 24.2 |
| .644 | 23.96 ± 0.21 | 12 | 7 | .642 | 14.7 | 17.0 ± 1.1 | 14.9 ± 1.4 | 4.4 | 21.4 | 19.3 |
| | | 12 | 24 | .642 | 27.9 | 17.4 ± 0.6 | 16.2 ± 0.5 | 7.7 | 25.1 | 23.9 |
| | | 16 | 1 | .642 | 28.2 | 17.3 ± 0.4 | 15.8 ± 0.4 | 7.7 | 25.0 | 23.5 |
| | | 6 | 15 | .643 | 18.7 | 17.9 ± 0.6 | 17.1 ± 1.0 | 5.4 | 23.3 | 22.5 |
| | | 9 | 2 | .647 | 14.7 | 19.3 ± 0.3 | 19.7 ± 0.9 | 4.4 | 23.7 | 24.1 |
| | | 10 | 4 | .647 | 18.5 | 20.0 ± 0.8 | 19.7 ± 0.7 | 5.4 | 25.4 | 25.1 |
| | | 8 | 5 | .648 | 23.4 | 18.1 ± 0.3 | 17.0 ± 0.2 | 6.6 | 24.7 | 23.6 |
| .681 | 24.25 ± 0.36 | 12 | 8 | .679 | 16.6 | 21.1 ± 1.9 | 13.0 ± 1.7 | 4.9 | 26.0 | 17.9 |
| | | 9 | 3 | .681 | 16.5 | 19.4 ± 0.3 | 18.4 ± 0.3 | 4.9 | 24.3 | 23.3 |
| | | 10 | 5 | .681 | 20.5 | 19.9 ± 0.7 | 17.8 ± 0.8 | 5.9 | 25.8 | 23.7 |
| | | 11 | 15 | .681 | 25.3 | 19.1 ± 0.6 | 18.2 ± 0.5 | 7.1 | 26.2 | 25.3 |
| | | 12 | 21 | .682 | 26.2 | 16.5 ± 0.7 | 17.7 ± 0.9 | 7.2 | 23.7 | 24.9 |
| .695 | 24.32 ± 0.28 | 3 | 13 | .689 | 17.2 | 18.5 ± 0.2 | 18.6 ± 0.4 | 5.0 | 23.5 | 23.6 |
| | | 6 | 14 | .690 | 22.2 | 18.9 ± 0.8 | 17.7 ± 0.8 | 6.3 | 25.2 | 24.0 |
| | | 12 | 22 | .694 | 27.3 | 16.0 ± 0.8 | 15.9 ± 1.0 | 7.5 | 23.5 | 23.4 |
| | | 4 | 19 | .699 | 27.7 | 17.5 ± 0.3 | 17.9 ± 0.3 | 7.6 | 25.1 | 25.5 |
| | | 11 | 16 | .702 | 28.0 | 17.7 ± 0.5 | 17.0 ± 0.7 | 7.7 | 25.4 | 24.7 |
| .726 | 24.44 ± 0.17 | 12 | 9 | .721 | 19.3 | 17.0 ± 0.9 | 19.0 ± 0.9 | 5.6 | 22.6 | 24.6 |
| | | 17 | 7 | .725 | 32.2 | 18.0 ± 1.2 | 14.9 ± 1.4 | 8.5 | 26.5 | 23.4 |
| | | 10 | 6 | .726 | 25.1 | 17.9 ± 0.4 | 17.8 ± 0.4 | 7.0 | 24.9 | 24.8 |
| | | 3 | 12 | .728 | 20.6 | 18.5 ± 0.3 | 18.4 ± 0.5 | 5.9 | 24.4 | 24.3 |
| | | 9 | 4 | .731 | 20.4 | 18.2 ± 0.4 | 18.0 ± 0.8 | 5.9 | 24.1 | 23.9 |
| .735 | 24.89 ± 0.35 | 11 | 17 | .734 | 32.3 | 17.3 ± 0.5 | 18.1 ± 0.6 | 8.6 | 25.9 | 26.7 |
| | | 12 | 23 | .735 | 33.1 | 15.2 ± 0.4 | 15.9 ± 0.5 | 8.7 | 23.9 | 24.6 |
| | | 2 | 28 | .735 | 20.4 | 18.9 ± 0.6 | 18.4 ± 0.6 | 5.9 | 24.8 | 24.3 |
| | | 6 | 13 | .741 | 27.4 | 17.6 ± 0.7 | 16.2 ± 0.7 | 7.5 | 25.1 | 23.7 |
| .758 | 25.53 ± 0.25 | 3 | 11 | .750 | 22.3 | 17.9 ± 0.4 | 18.2 ± 0.7 | 6.4 | 24.3 | 24.6 |
| | | 8 | 6 | .758 | 36.3 | 16.8 ± 0.3 | 16.0 ± 0.2 | 9.4 | 26.2 | 25.4 |
| | | 17 | 6 | .762 | 38.0 | 15.4 ± 0.6 | 14.6 ± 0.7 | 9.7 | 25.1 | 24.3 |
| | | 10 | 7 | .763 | 29.6 | 18.8 ± 0.5 | 18.5 ± 0.5 | 8.0 | 26.8 | 26.5 |
| .776 | 24.41 ± 0.14 | 12 | 10 | .773 | 24.0 | 17.4 ± 2.6 | 17.0 ± 2.8 | 6.8 | 24.2 | 23.8 |
| | | 9 | 5 | .779 | 25.7 | 17.5 ± 0.2 | 16.9 ± 0.3 | 7.1 | 24.6 | 24.0 |
| .791 | 26.58 ± 0.20 | 6 | 11 | .789 | 32.2 | 18.4 ± 0.3 | 18.4 ± 0.4 | 8.6 | 27.0 | 27.0 |
| | | 10 | 8 | .789 | 31.7 | 18.2 ± 1.1 | 19.2 ± 0.9 | 8.5 | 26.7 | 27.7 |
| | | 6 | 12 | .790 | 32.8 | 16.7 ± 0.3 | 18.6 ± 0.5 | 8.7 | 25.4 | 27.3 |
| | | 12 | 11 | .790 | 26.3 | 18.0 ± 2.8 | 21.2 ± 2.6 | 7.3 | 25.3 | 28.5 |
| | | 9 | 6 | .795 | 26.7 | 19.7 ± 0.6 | 19.0 ± 0.7 | 7.4 | 27.1 | 26.4 |
| | | 2 | 29 | .796 | 26.7 | 19.2 ± 0.4 | 19.2 ± 0.4 | 7.4 | 26.6 | 26.6 |
| .810 | 27.76 ± 0.48 | 17 | 5 | .808 | 46.0 | 14.6 ± 0.4 | 15.7 ± 0.5 | 11.1 | 25.7 | 26.8 |
| | | 9 | 7 | .810 | 28.5 | 21.1 ± 0.6 | 22.0 ± 1.3 | 7.8 | 28.9 | 29.8 |

TABLE VI.- ZERO-LIFT WING-FUSELAGE PITCHING-MOMENT COEFFICIENTS

| Group M | Group $\frac{}{c_{m_0}}$ | Flight | Run | M | $c_{m_0}$ (method I) | $c_{m_0}$ (method I corrected for zero shift) | $\epsilon c_{m_0}$ (method I) | $c_{m_0}$ (method II) | $\epsilon c_{m_0}$ (method II) |
|---|---|---|---|---|---|---|---|---|---|
| 0.429 | -0.0371 ± 0.0023 | 11 | 24 | 0.427 | -0.0051 | -0.0285 | ±0.0057 | -0.0402 | ±0.0063 |
| | | 12 | 28 | .427 | -.0173 | -.0313 | ±.0091 | -.0379 | ±.0083 |
| | | 16 | 5 | .428 | .0704 | -.0319 | ±.0019 | -.0389 | ±.0027 |
| | | 16 | 6 | .433 | .0532 | -.0358 | ±.0013 | -.0546 | ±.0028 |
| .486 | -0.0365 ± 0.0012 | 12 | 27 | .482 | -.0266 | -.0307 | ±.0057 | -.0326 | ±.0033 |
| | | 16 | 4 | .482 | .0501 | -.0361 | ±.0021 | -.0401 | ±.0046 |
| | | 12 | 17 | .483 | -.0924 | -.0387 | ±.0098 | -.0448 | ±.0114 |
| | | 4 | 21 | .486 | -.0227 | -.0415 | ±.0035 | -.0397 | ±.0049 |
| | | 11 | 11 | .495 | .0065 | -.0264 | ±.0069 | -.0354 | ±.0089 |
| .541 | -0.0426 ± 0.0019 | 12 | 18 | .532 | -.0866 | -.0388 | ±.0054 | -.0413 | ±.0057 |
| | | 11 | 12 | .542 | -.0081 | -.0301 | ±.0024 | -.0358 | ±.0030 |
| | | 16 | 3 | .542 | .0383 | -.0394 | ±.0018 | -.0452 | ±.0025 |
| | | 12 | 26 | .543 | -.0466 | -.0441 | ±.0021 | -.0452 | ±.0016 |
| | | 8 | 4 | .544 | .1286 | -.0449 | ±.0045 | -.0515 | ±.0019 |
| .595 | -0.0459 ± 0.0016 | 12 | 6 | .584 | .1379 | -.0554 | ±.0043 | -.0823 | ±.0092 |
| | | 4 | 20 | .591 | -.0563 | -.0532 | ±.0027 | -.0454 | ±.0025 |
| | | 12 | 25 | .595 | -.0597 | -.0452 | ±.0027 | -.0435 | ±.0016 |
| | | 11 | 13 | .597 | -.0212 | -.0415 | ±.0013 | -.0429 | ±.0018 |
| | | 10 | 3 | .598 | .1851 | -.0492 | ±.0051 | -.0534 | ±.0025 |
| | | 9 | 1 | .598 | .2981 | -.0507 | ±.0070 | -.0682 | ±.0034 |
| | | 16 | 2 | .599 | .0242 | -.0455 | ±.0014 | -.0496 | ±.0029 |
| | | 12 | 19 | .600 | -.0963 | -.0546 | ±.0039 | -.0379 | ±.0023 |
| .635 | -0.0495 ± 0.0026 | 3 | 14 | .631 | .0069 | -.0595 | ±.0014 | -.0465 | ±.0020 |
| | | 2 | 27 | .636 | -.0229 | -.0478 | ±.0033 | -.0551 | ±.0023 |
| | | 11 | 14 | .636 | -.0429 | -.0446 | ±.0024 | -.0431 | ±.0017 |
| | | 12 | 20 | .637 | -.0954 | -.0485 | ±.0045 | -.0392 | ±.0022 |
| .644 | -0.0445 ± 0.0011 | 12 | 7 | .642 | .0914 | -.0678 | ±.0044 | -.0753 | ±.0074 |
| | | 12 | 24 | .642 | -.0638 | -.0457 | ±.0028 | -.0448 | ±.0013 |
| | | 16 | 1 | .642 | .0203 | -.0417 | ±.0007 | -.0445 | ±.0011 |
| | | 6 | 15 | .643 | -.0201 | -.0489 | ±.0033 | -.0596 | ±.0038 |
| | | 9 | 2 | .647 | .2108 | -.0597 | ±.0102 | -.0562 | ±.0044 |
| | | 10 | 4 | .647 | .1270 | -.0417 | ±.0038 | -.0403 | ±.0032 |
| | | 8 | 5 | .648 | .0674 | -.0436 | ±.0014 | -.0472 | ±.0010 |
| .681 | -0.0478 ± 0.0018 | 12 | 8 | .679 | .0766 | -.0447 | ±.0073 | -.0771 | ±.0079 |
| | | 9 | 3 | .681 | .1566 | -.0539 | ±.0053 | -.0553 | ±.0017 |
| | | 10 | 5 | .681 | .0962 | -.0419 | ±.0025 | -.0478 | ±.0033 |
| | | 11 | 15 | .681 | -.0462 | -.0441 | ±.0027 | -.0462 | ±.0015 |
| | | 12 | 21 | .682 | -.0942 | -.0470 | ±.0043 | -.0418 | ±.0025 |
| .695 | -0.0523 ± 0.0015 | 3 | 13 | .689 | -.0120 | -.0614 | ±.0014 | -.0585 | ±.0023 |
| | | 6 | 14 | .690 | -.0240 | -.0517 | ±.0040 | -.0529 | ±.0031 |
| | | 12 | 22 | .694 | -.0916 | -.0505 | ±.0049 | -.0487 | ±.0028 |
| | | 4 | 19 | .699 | -.0615 | -.0530 | ±.0018 | -.0496 | ±.0009 |
| | | 11 | 16 | .702 | -.0550 | -.0485 | ±.0021 | -.0483 | ±.0017 |
| .726 | -0.0620 ± 0.0013 | 12 | 9 | .721 | .0338 | -.0615 | ±.0029 | -.0514 | ±.0036 |
| | | 17 | 7 | .725 | -.0118 | -.0513 | ±.0037 | -.0556 | ±.0037 |
| | | 10 | 6 | .726 | .0352 | -.0612 | ±.0009 | -.0593 | ±.0016 |
| | | 3 | 12 | .728 | -.0217 | -.0651 | ±.0013 | -.0633 | ±.0022 |
| | | 9 | 4 | .731 | .1017 | -.0728 | ±.0029 | -.0711 | ±.0035 |
| .736 | -0.0586 ± 0.0016 | 11 | 17 | .734 | -.0632 | -.0592 | ±.0023 | -.0557 | ±.0013 |
| | | 12 | 23 | .735 | -.0908 | -.0598 | ±.0027 | -.0547 | ±.0015 |
| | | 2 | 28 | .735 | -.0573 | -.0632 | ±.0039 | -.0645 | ±.0026 |
| | | 6 | 13 | .741 | -.0345 | -.0654 | ±.0037 | -.0674 | ±.0024 |
| .758 | -0.0637 ± 0.0007 | 3 | 11 | .750 | -.0275 | -.0777 | ±.0027 | -.0725 | ±.0028 |
| | | 8 | 6 | .758 | .0168 | -.0634 | ±.0004 | -.0628 | ±.0005 |
| | | 17 | 6 | .762 | -.0263 | -.0664 | ±.0021 | -.0653 | ±.0019 |
| | | 10 | 7 | .763 | .0115 | -.0652 | ±.0010 | -.0629 | ±.0017 |
| .776 | -0.0809 ± 0.0003 | 12 | 10 | .773 | -.0036 | -.0789 | ±.0088 | -.0774 | ±.0098 |
| | | 9 | 5 | .779 | .0460 | -.0807 | ±.0015 | -.0812 | ±.0016 |
| .791 | -0.0770 ± 0.0010 | 6 | 11 | .789 | -.0360 | -.0733 | ±.0012 | -.0772 | ±.0011 |
| | | 10 | 8 | .789 | -.0065 | -.0733 | ±.0029 | -.0659 | ±.0028 |
| | | 6 | 12 | .790 | -.0428 | -.0791 | ±.0020 | -.0772 | ±.0016 |
| | | 12 | 11 | .790 | .0024 | -.0802 | ±.0104 | -.0675 | ±.0068 |
| | | 9 | 6 | .795 | .0315 | -.0801 | ±.0022 | -.0798 | ±.0027 |
| | | 2 | 29 | .796 | -.0760 | -.0838 | ±.0036 | -.0815 | ±.0014 |
| .810 | -0.0779 ± 0.0023 | 17 | 5 | .808 | -.0374 | -.0760 | ±.0017 | -.0700 | ±.0012 |
| | | 9 | 7 | .810 | .0201 | -.0866 | ±.0021 | -.0785 | ±.0044 |
| | | 10 | 9 | .812 | -.0102 | -.0826 | ±.0012 | -.0795 | ±.0013 |
| | | 12 | 12 | .812 | -.0304 | -.0848 | ±.0075 | -.0715 | ±.0058 |

TABLE VII.- RADIUS-OF-GYRATION DATA

| Flight | Run | $k_{y_f}^2$ (method II) | $\epsilon_{k_{y_f}}^2$ (method II) | $k_{y_f}^2$ (method I) | $\epsilon_{k_{y_f}}^2$ (method I) | $(k_{y_f}^2)_{av}$ (methods I and II) | $(k_{y_f}^2)_{calc}$ | $\frac{\bar{q}_R}{W}$ | $\Delta k_{y_f}^2$ |
|---|---|---|---|---|---|---|---|---|---|
| 2 | 27 | 370.8 | ±3.2 | 404.9 | ±12.9 | 387.8 | 363.0 | 1.208 × 10⁻⁴ | 24.8 |
|   | 28 | 357.8 | ±4.0 | 385.9 | ±11.5 | 371.8 | 360.7 | 1.834 | 11.1 |
|   | 29 | 348.5 | ±3.7 | 394.1 | ±10.8 | 371.3 | 358.3 | 2.380 | 13.0 |
| 3 | 11 | 359.1 | ±4.5 | 371.8 | ±10.6 | 365.4 | 367.5 | 1.854 | -2.1 |
|   | 12 | 377.3 | ±2.5 | 394.7 | ±7.6 | 386.0 | 367.9 | 1.715 | 18.1 |
|   | 13 | 351.6 | ±4.6 | 382.8 | ±9.0 | 367.2 | 369.2 | 1.435 | -2.0 |
|   | 14 | 404.2 | ±2.8 | 395.2 | ±7.3 | 399.7 | 369.9 | 1.168 | 29.8 |
| 4 | 19 | 317.0 | ±4.5 | 337.6 | ±5.9 | 327.3 | 335.1 | 2.544 | -7.8 |
|   | 20 | 341.5 | ±3.2 | 343.9 | ±6.9 | 342.7 | 338.3 | 1.702 | 4.4 |
|   | 21 | 340.8 | ±3.8 | 367.5 | ±8.5 | 354.2 | 340.6 | 1.098 | 13.6 |
| 6 | 11 | 318.0 | ±2.7 | 365.2 | ±8.6 | 341.6 | 343.7 | 2.960 | -2.1 |
|   | 12 | 314.1 | ±3.0 | 308.9 | ±6.8 | 311.5 | 343.8 | 3.017 | -32.3 |
|   | 13 | 306.2 | ±3.0 | 331.7 | ±10.4 | 319.0 | 345.6 | 2.528 | -26.6 |
|   | 14 | 340.3 | ±3.9 | 362.4 | ±13.6 | 351.3 | 348.1 | 2.052 | 3.2 |
|   | 15 | 313.5 | ±4.6 | 341.3 | ±11.0 | 327.4 | 349.3 | 1.738 | -21.9 |
| 8 | 4 | 304.3 | ±3.4 | 332.3 | ±8.9 | 318.3 | 351.7 | 1.242 | -33.4 |
|   | 5 | 315.3 | ±1.8 | 337.2 | ±5.6 | 326.2 | 349.4 | 1.880 | -23.2 |
|   | 6 | 290.7 | ±1.5 | 326.3 | ±5.0 | 308.5 | 345.4 | 2.927 | -36.9 |
| 9 | 1 | 344.3 | ±3.2 | 370.4 | ±6.2 | 357.3 | 363.9 | .963 | -6.6 |
|   | 2 | 335.0 | ±4.7 | 360.4 | ±12.0 | 347.7 | 362.7 | 1.165 | -15.0 |
|   | 3 | 307.7 | ±3.6 | 360.1 | ±8.0 | 333.9 | 362.1 | 1.308 | -28.2 |
|   | 4 | 337.1 | ±4.9 | 344.3 | ±5.9 | 340.7 | 361.2 | 1.623 | -20.5 |
|   | 5 | 344.6 | ±2.9 | 333.0 | ±5.5 | 338.8 | 359.8 | 2.049 | -21.0 |
|   | 6 | 348.5 | ±5.8 | 368.5 | ±14.4 | 358.5 | 359.7 | 2.133 | -1.2 |
|   | 7 | 360.6 | ±9.9 | 362.8 | ±15.7 | 361.7 | 359.1 | 2.282 | 2.6 |
| 10 | 3 | 347.0 | ±2.0 | 351.8 | ±8.5 | 349.4 | 360.5 | 1.219 | -11.1 |
|   | 4 | 364.0 | ±3.1 | 380.0 | ±10.3 | 372.0 | 359.7 | 1.462 | 12.3 |
|   | 5 | 334.8 | ±3.0 | 352.6 | ±8.1 | 343.7 | 359.3 | 1.623 | -15.6 |
|   | 6 | 329.6 | ±2.0 | 334.9 | ±4.9 | 332.2 | 357.8 | 1.990 | -25.6 |
|   | 7 | 332.3 | ±2.4 | 347.1 | ±6.4 | 339.7 | 356.9 | 2.360 | -17.2 |
|   | 8 | 328.2 | ±3.4 | 330.2 | ±11.5 | 329.2 | 356.5 | 2.552 | -27.3 |
|   | 9 | 327.4 | ±2.1 | 343.1 | ±5.8 | 335.2 | 355.8 | 2.794 | -20.6 |
| 11 | 11 | 336.1 | ±4.8 | 361.5 | ±13.0 | 348.8 | 356.9 | 1.172 | -8.1 |
|   | 12 | 334.6 | ±2.8 | 362.7 | ±6.6 | 348.6 | 356.0 | 1.433 | -7.4 |
|   | 13 | 336.5 | ±2.7 | 358.4 | ±5.6 | 347.4 | 355.7 | 1.742 | -8.3 |
|   | 14 | 327.2 | ±4.3 | 331.5 | ±7.2 | 329.3 | 354.5 | 2.037 | -25.2 |
|   | 15 | 328.6 | ±2.4 | 343.8 | ±8.7 | 336.2 | 353.3 | 2.334 | -17.1 |
|   | 16 | 319.2 | ±2.6 | 332.4 | ±5.7 | 325.8 | 352.5 | 2.597 | -26.7 |
|   | 17 | 303.7 | ±2.3 | 309.8 | ±5.8 | 306.7 | 350.5 | 3.005 | -43.8 |
|   | 24 | 355.2 | ±5.0 | 375.4 | ±18.1 | 365.3 | 359.5 | 1.099 | 5.8 |
| 12 | 6 | 318.0 | ±3.8 | 334.4 | ±7.5 | 326.2 | 350.1 | 1.022 | -23.9 |
|   | 7 | 319.1 | ±3.2 | 329.7 | ±8.5 | 324.4 | 349.3 | 1.222 | -24.9 |
|   | 8 | 314.9 | ±2.5 | 336.7 | ±11.9 | 325.8 | 348.7 | 1.384 | -22.9 |
|   | 9 | 326.9 | ±2.3 | 315.9 | ±7.7 | 321.4 | 347.4 | 1.614 | -26.0 |
|   | 10 | 308.6 | ±6.0 | 302.0 | ±16.6 | 305.3 | 346.3 | 2.015 | -41.0 |
|   | 11 | 330.1 | ±6.1 | 314.0 | ±7.3 | 322.0 | 345.5 | 2.214 | -23.5 |
|   | 12 | 327.9 | ±4.8 | 309.3 | ±10.6 | 318.6 | 344.2 | 2.443 | -25.6 |
|   | 17 | 331.6 | ±3.6 | 338.7 | ±8.2 | 335.2 | 349.3 | 1.029 | -14.1 |
|   | 18 | 334.1 | ±2.6 | 337.1 | ±6.0 | 335.6 | 348.4 | 1.270 | -12.8 |
|   | 19 | 340.5 | ±1.4 | 323.3 | ±5.2 | 331.9 | 347.1 | 1.658 | -15.2 |
|   | 20 | 330.4 | ±1.1 | 317.4 | ±6.1 | 323.9 | 346.1 | 1.909 | -22.2 |
|   | 21 | 321.3 | ±2.3 | 315.1 | ±6.4 | 318.2 | 344.7 | 2.257 | -26.5 |
|   | 22 | 307.7 | ±2.7 | 308.4 | ±7.6 | 308.0 | 344.8 | 2.358 | -36.8 |
|   | 23 | 313.5 | ±1.7 | 310.5 | ±4.5 | 312.0 | 343.4 | 2.868 | -31.4 |
|   | 24 | 294.3 | ±1.6 | 311.2 | ±6.0 | 302.7 | 336.2 | 2.511 | -33.5 |
|   | 25 | 309.9 | ±1.5 | 313.2 | ±5.1 | 311.5 | 337.8 | 2.124 | -26.3 |
|   | 26 | 312.0 | ±1.6 | 330.2 | ±4.8 | 321.1 | 339.5 | 1.736 | -18.4 |
|   | 27 | 311.1 | ±2.0 | 324.2 | ±8.6 | 317.6 | 341.3 | 1.553 | -23.7 |
|   | 28 | 314.1 | ±3.0 | 333.0 | ±11.0 | 323.5 | 341.8 | 1.034 | -18.3 |
| 16 | 1 | 332.9 | ±1.6 | 339.6 | ±4.5 | 336.2 | 354.1 | 2.408 | -17.9 |
|   | 2 | 324.1 | ±1.6 | 334.0 | ±5.8 | 329.0 | 354.3 | 2.055 | -25.3 |
|   | 3 | 342.9 | ±2.3 | 348.9 | ±7.2 | 345.9 | 354.8 | 1.630 | -8.9 |
|   | 4 | 347.2 | ±3.1 | 351.8 | ±6.4 | 349.5 | 356.7 | 1.276 | -8.2 |
|   | 5 | 349.8 | ±1.7 | 365.8 | ±5.4 | 357.8 | 358.5 | .996 | -.7 |
|   | 6 | 333.3 | ±1.5 | 362.0 | ±3.1 | 347.6 | 358.0 | 1.034 | -10.4 |
| 17 | 5 | 308.0 | ±2.4 | 298.3 | ±5.9 | 303.1 | 347.0 | 3.952 | -43.9 |
|   | 6 | 306.9 | ±2.7 | 315.2 | ±7.3 | 311.1 | 349.3 | 3.270 | -38.2 |
|   | 7 | 321.7 | ±3.9 | 339.3 | ±12.1 | 330.5 | 351.4 | 2.785 | -20.9 |
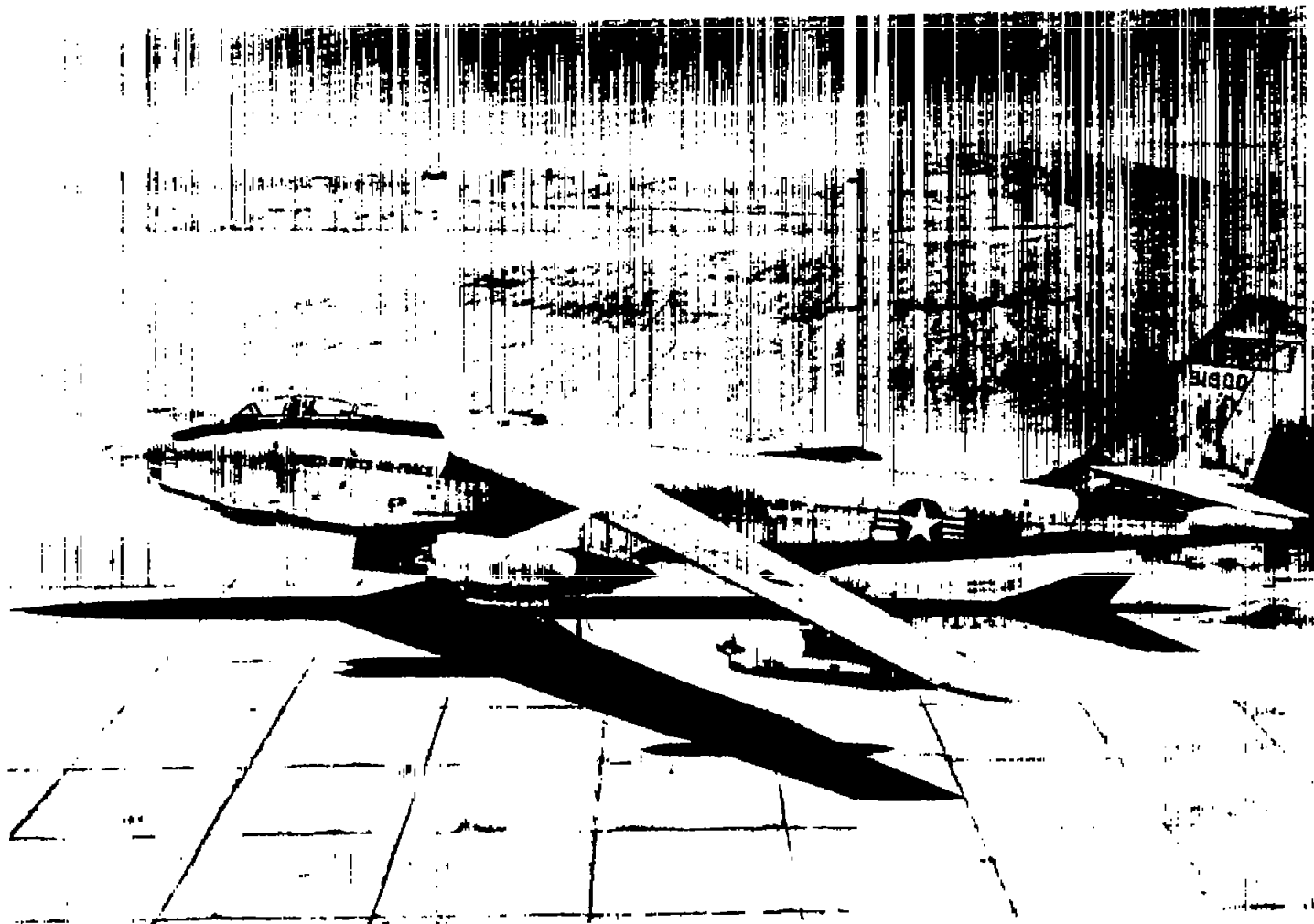
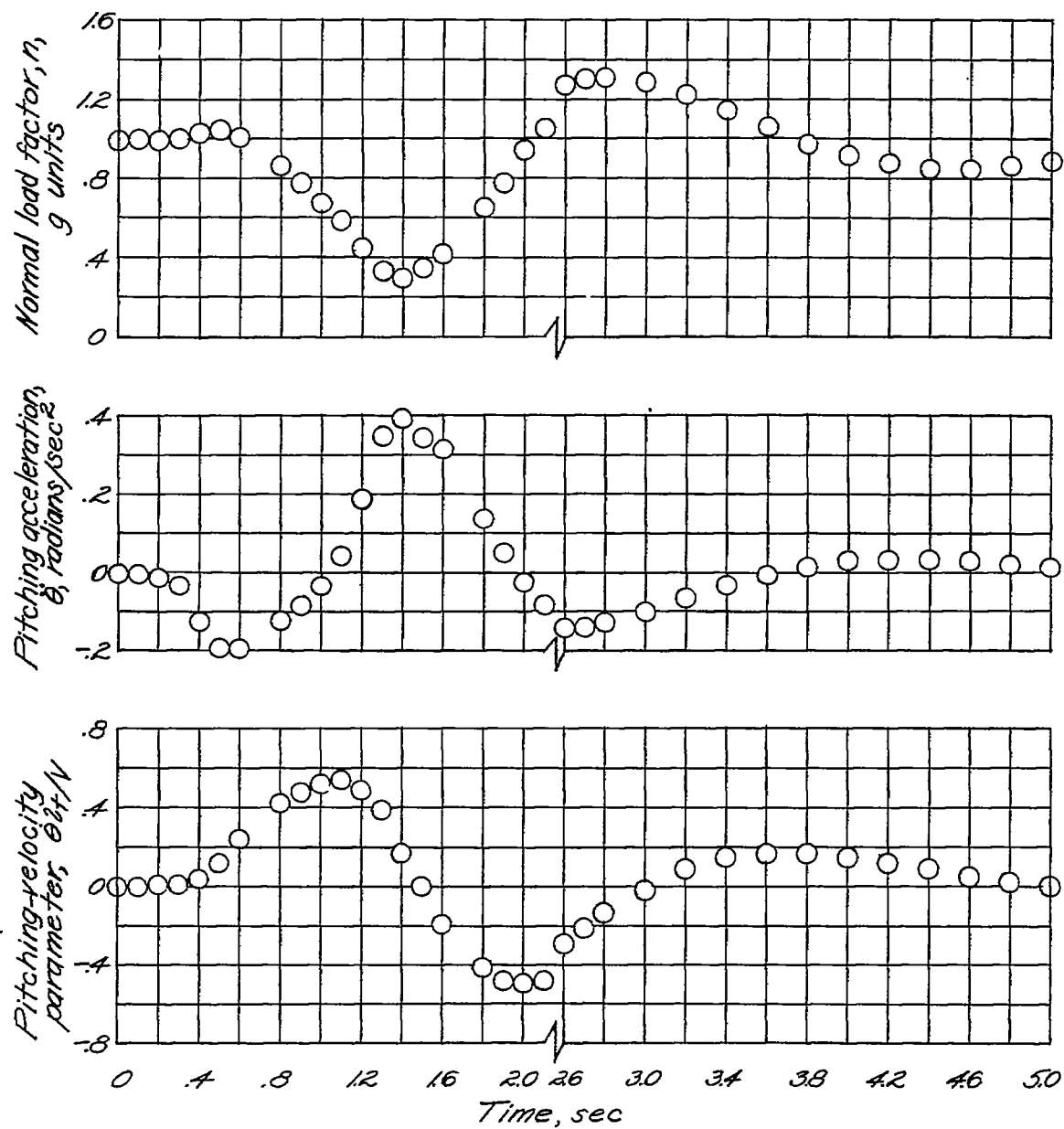Figure 1.- Side view of test airplane.    L-86692

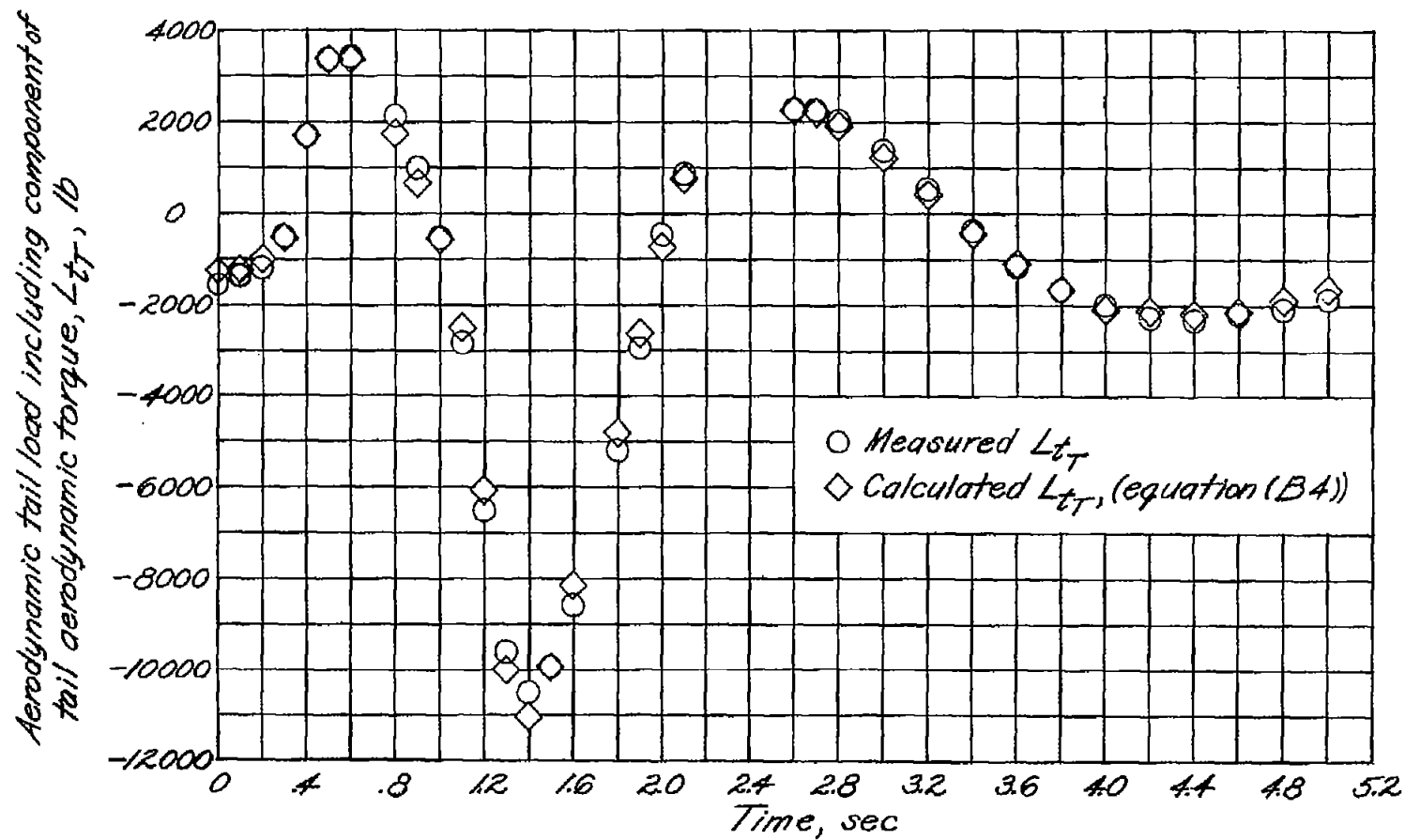Figure 2.- Time-history data for push-pull maneuver.

Figure 3.— Time histories of measured and calculated horizontal-tail aerodynamic loads for maneuver of figure 2.
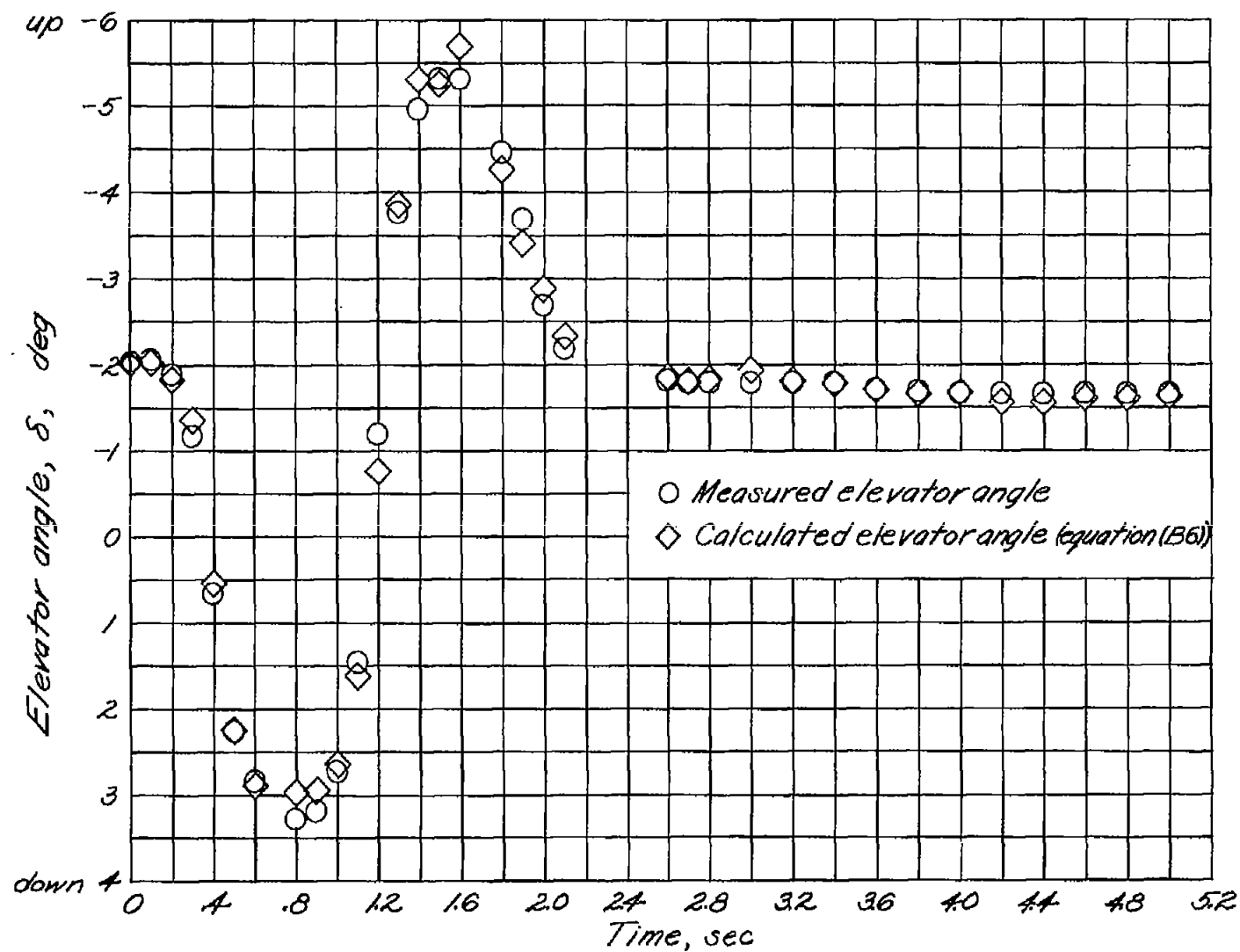
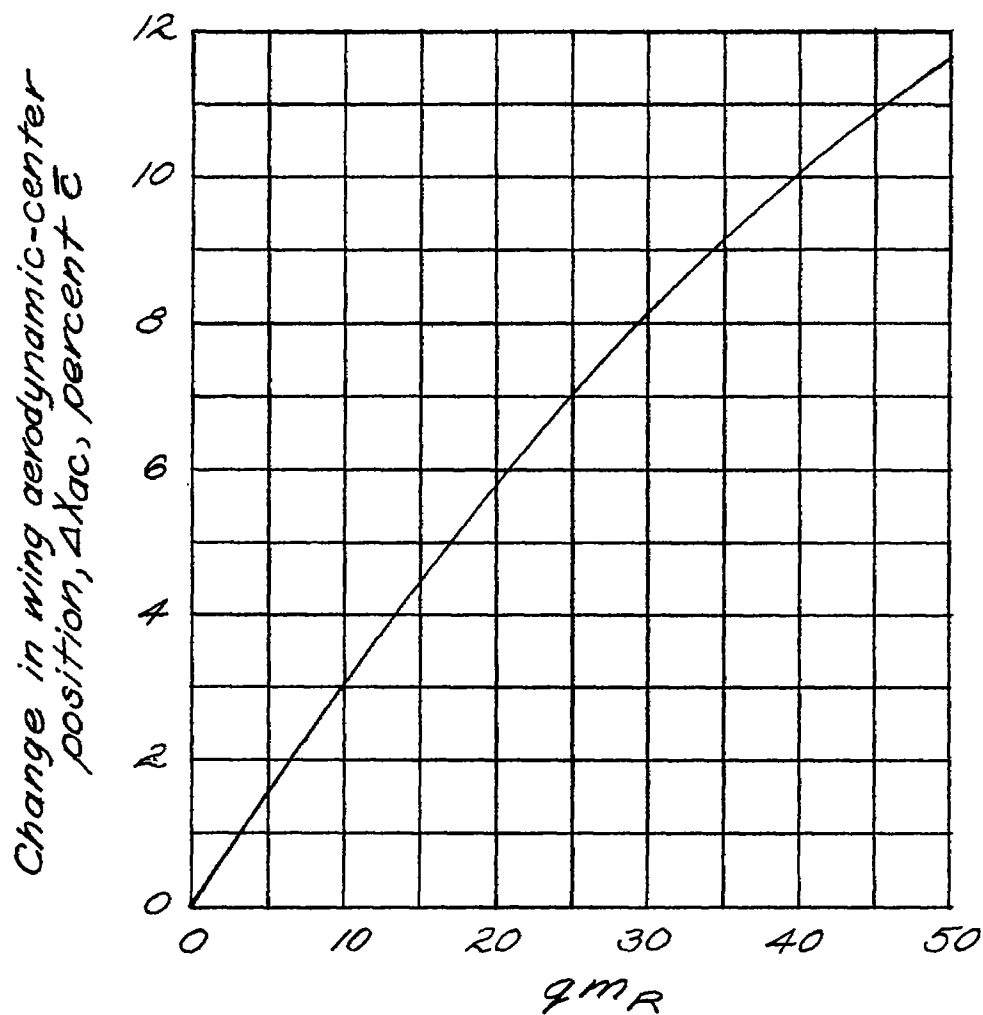Figure 4.- Time histories of measured and calculated elevator angles for maneuver of figure 2.

Figure 5.- Forward shift in wing aerodynamic-center position as a function of flexibility parameter from figure 4(c) of reference 5.
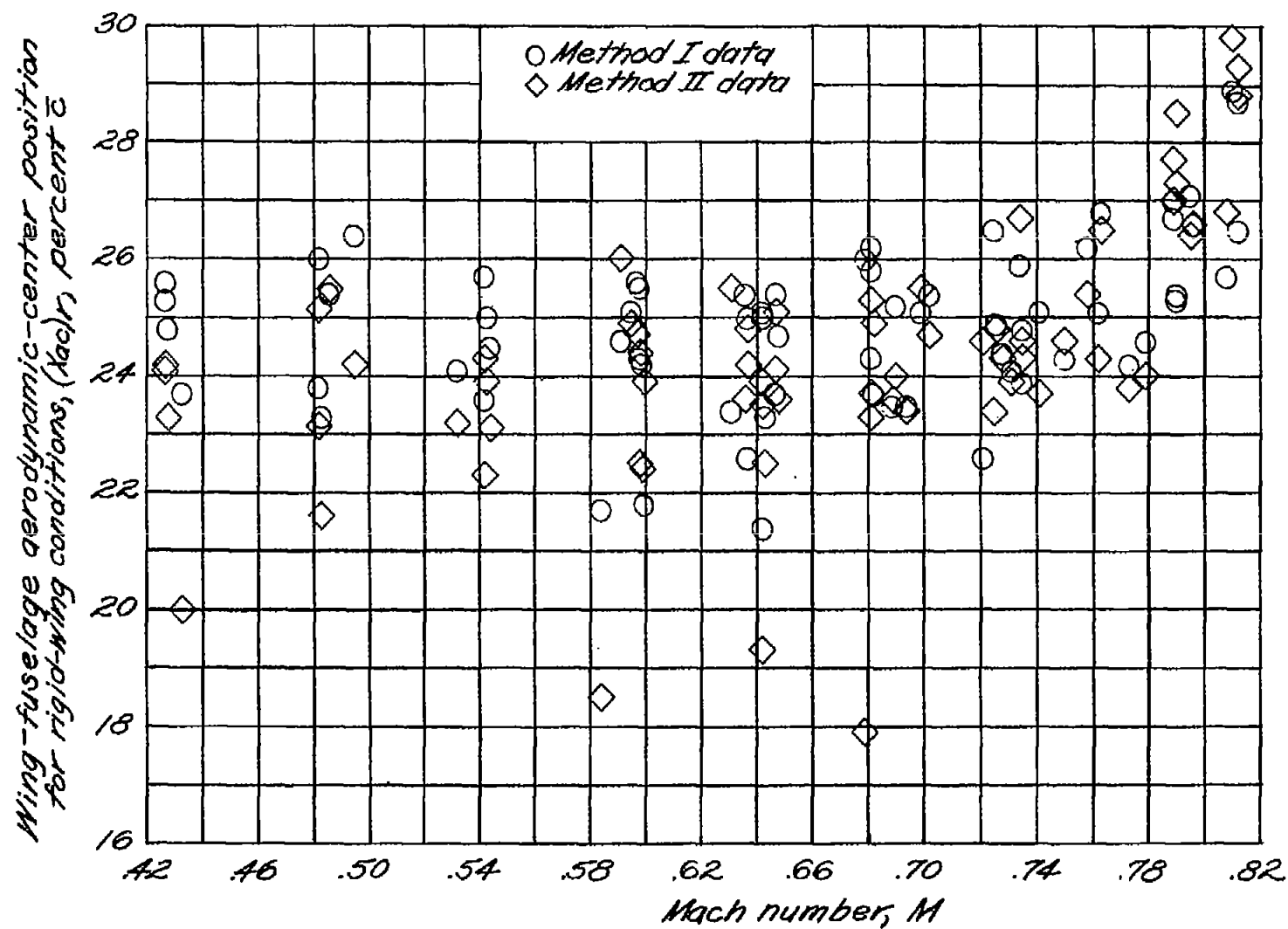
Figure 6.- Wing-fuselage aerodynamic-center data as extrapolated to rigid-wing conditions as a function of Mach number.
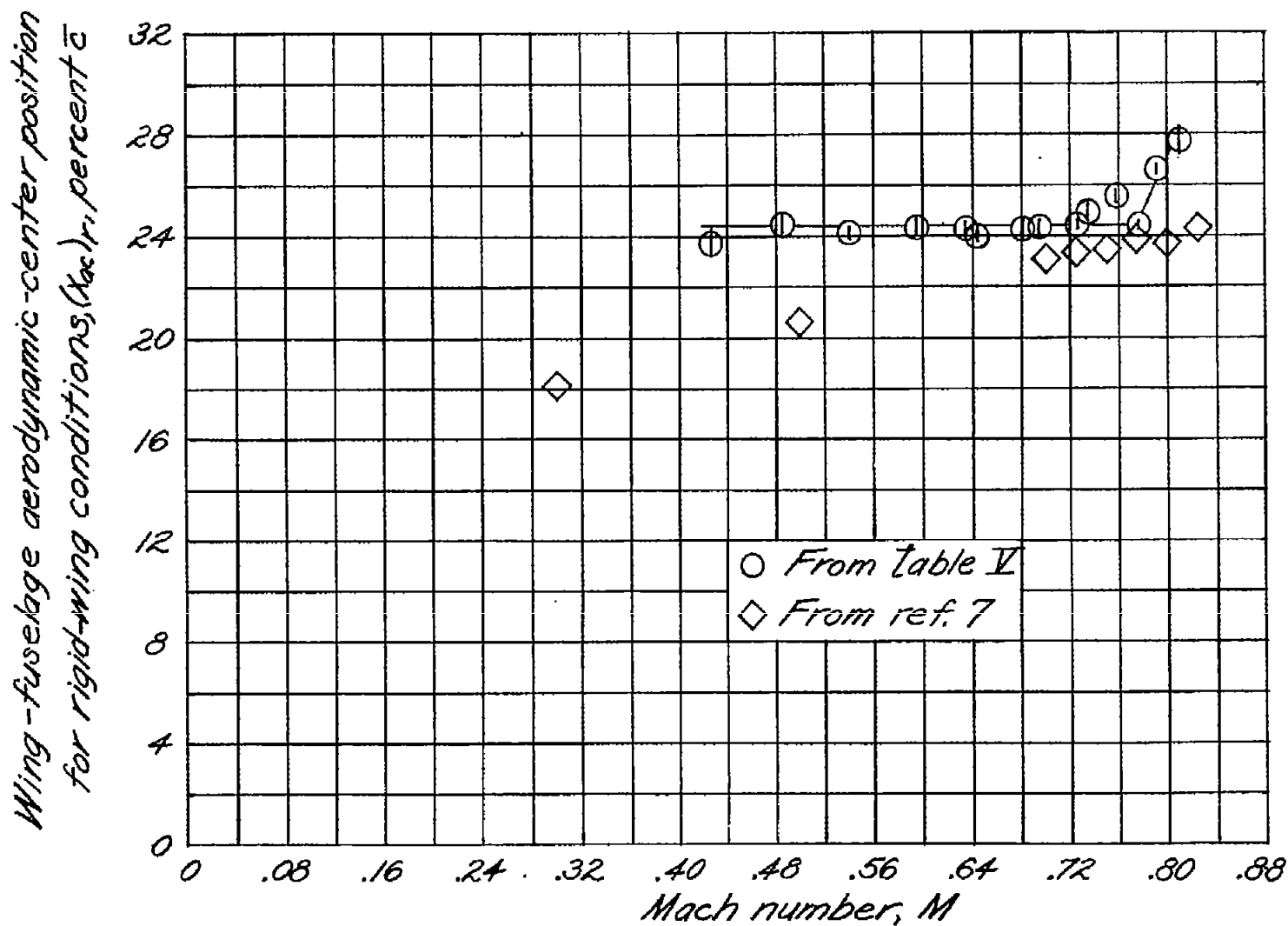
Figure 7.- Comparison of flight and wind-tunnel wing-fuselage aerodynamic-center positions for rigid-wing conditions.
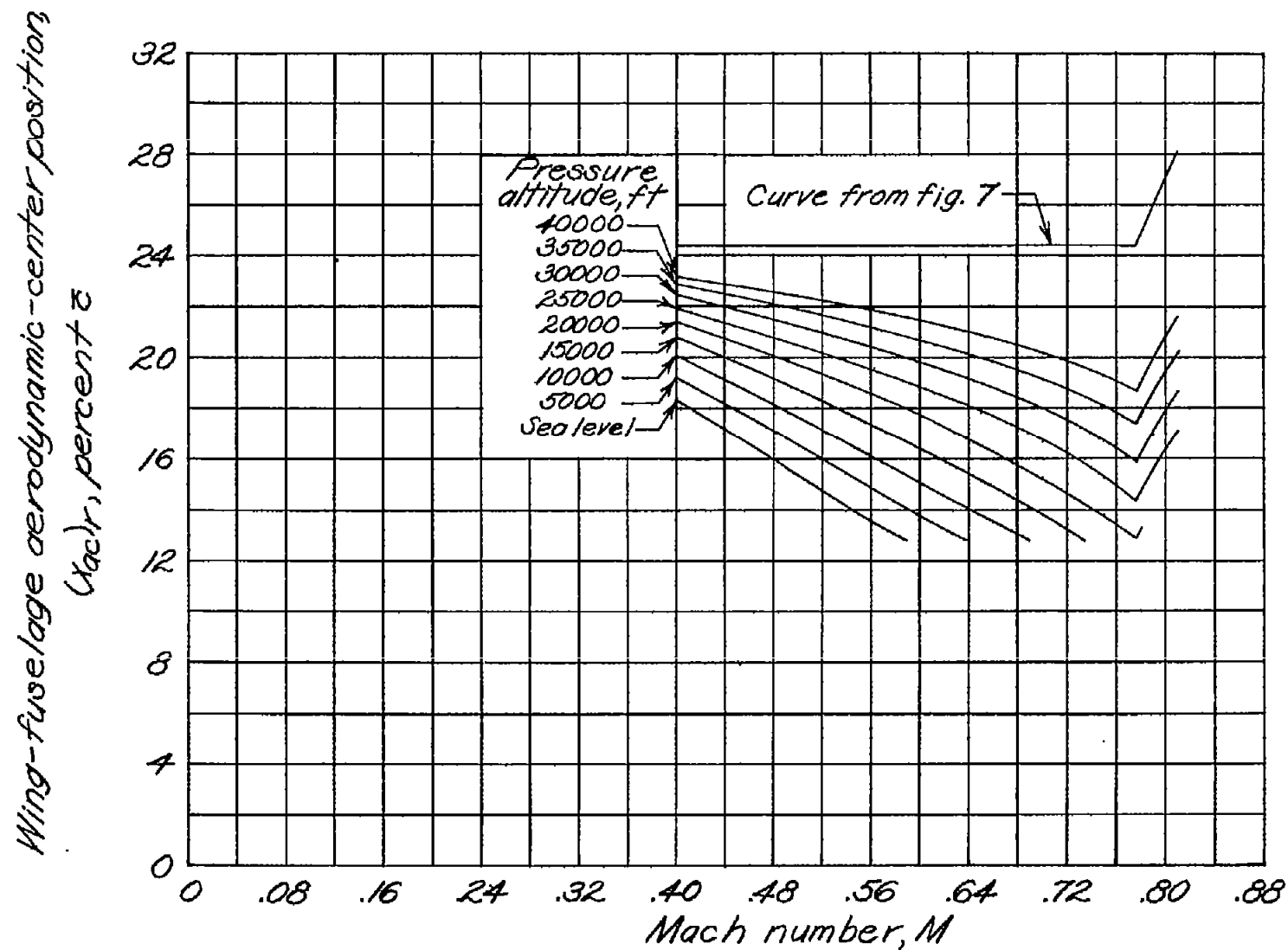
Figure 8.- Wing-fuselage aerodynamic-center position for flexible-wing conditions.
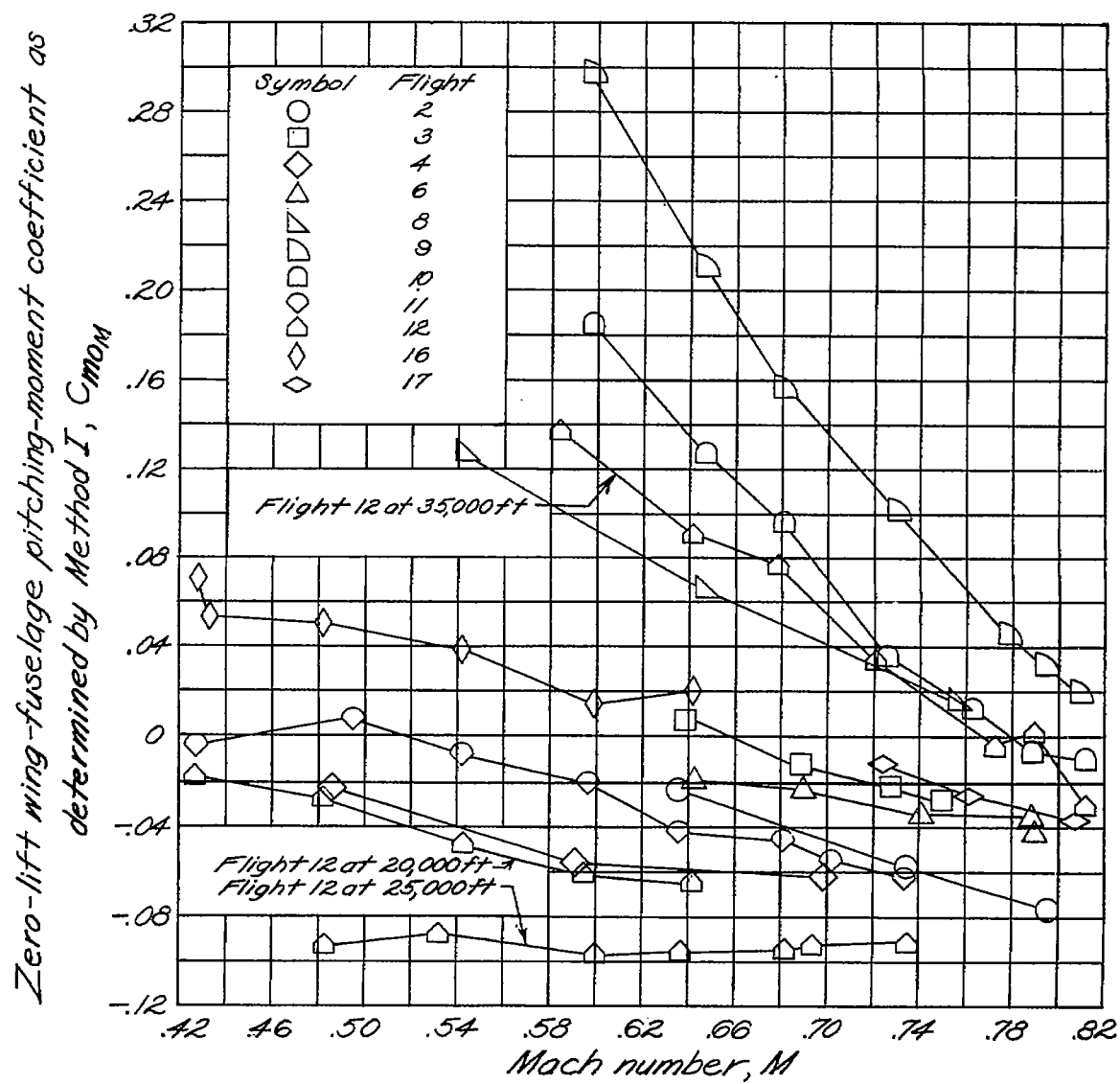
Figure 9.- Zero-lift wing-fuselage pitching-moment coefficient measured
by method I as a function of Mach number.
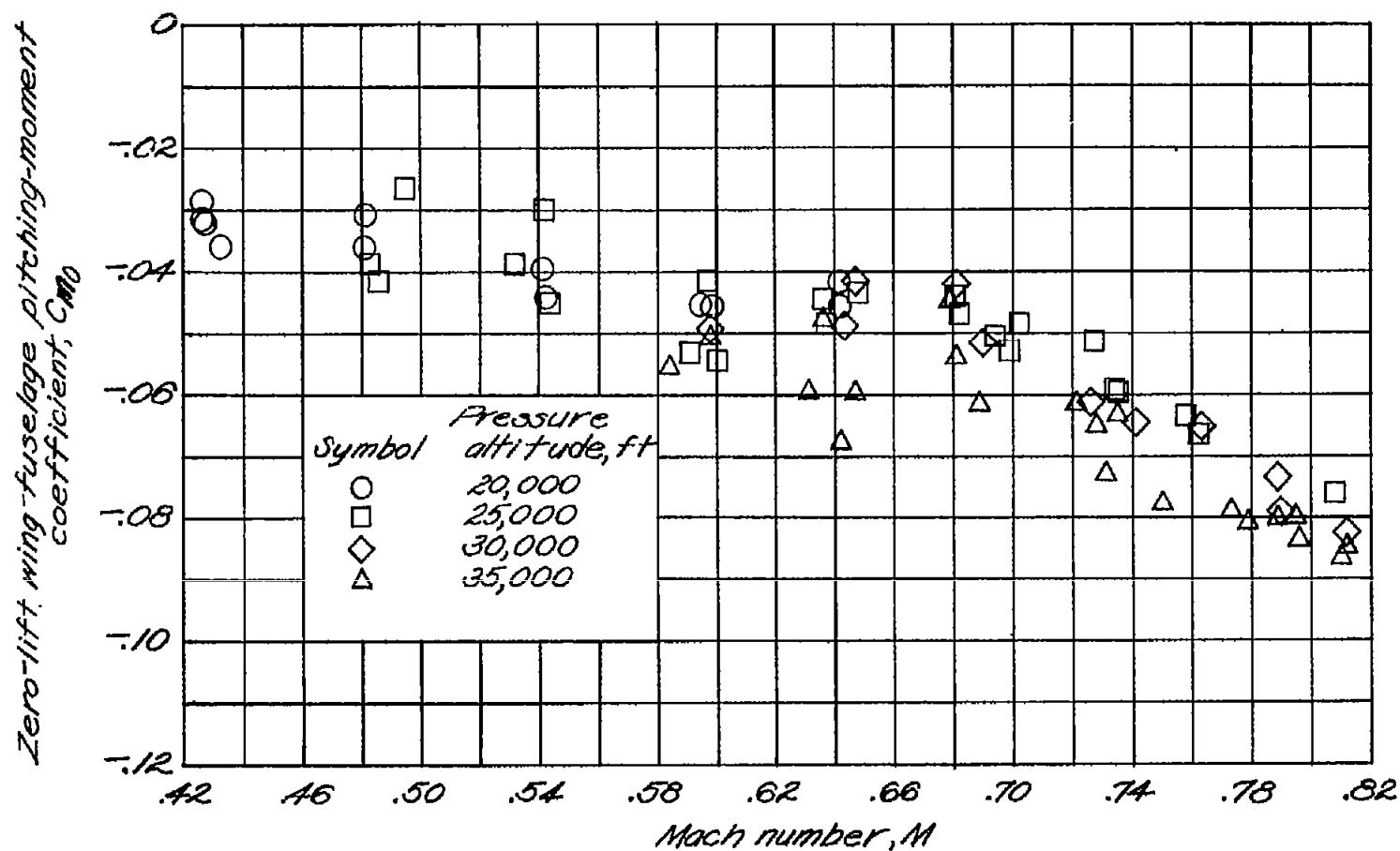
Figure 10.- Zero-lift wing-fuselage pitching-moment coefficients as obtained by method I and corrected for tail-load zero shifts.
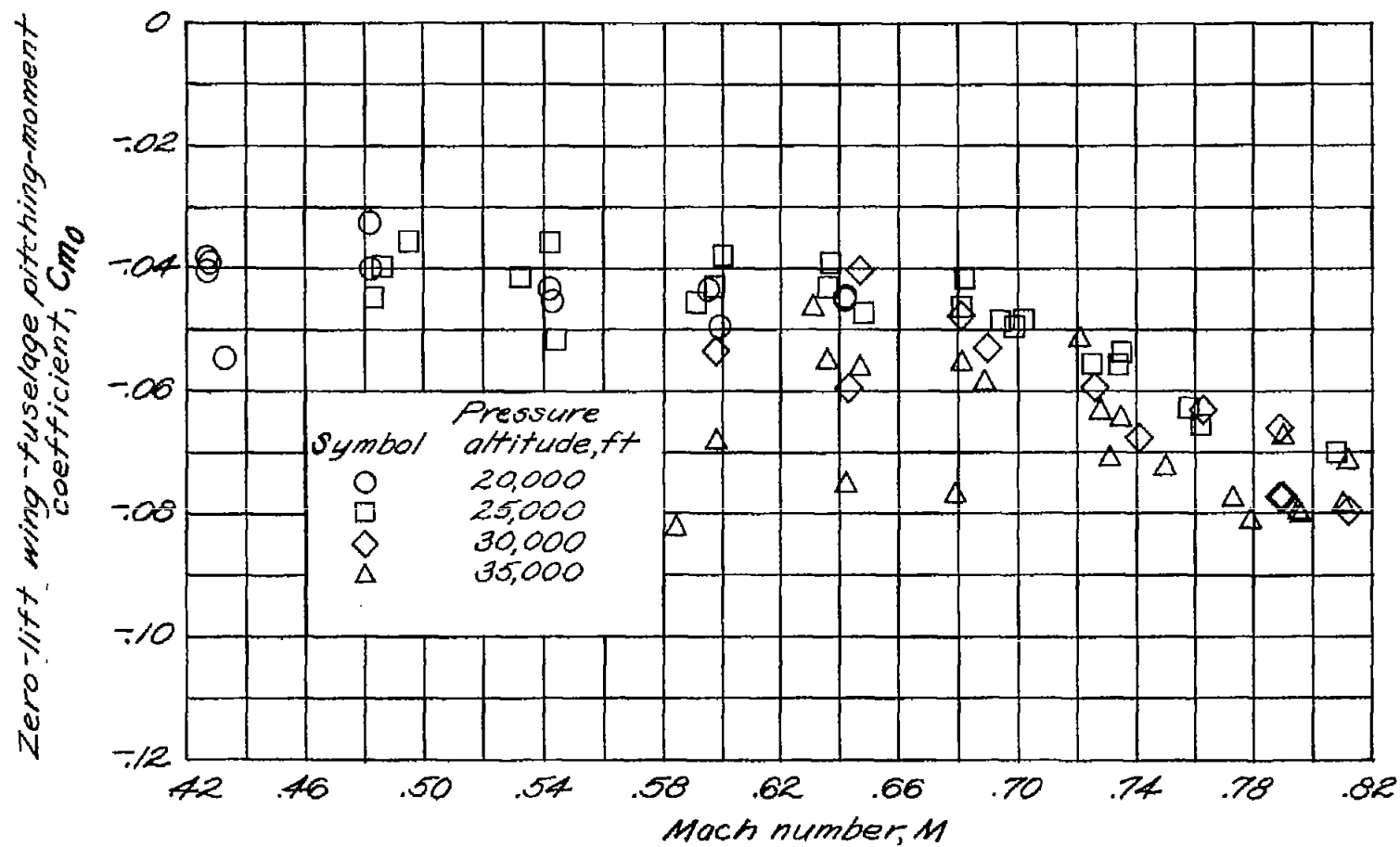
Figure 11.- Zero-lift wing-fuselage pitching-moment coefficients as obtained by method II.
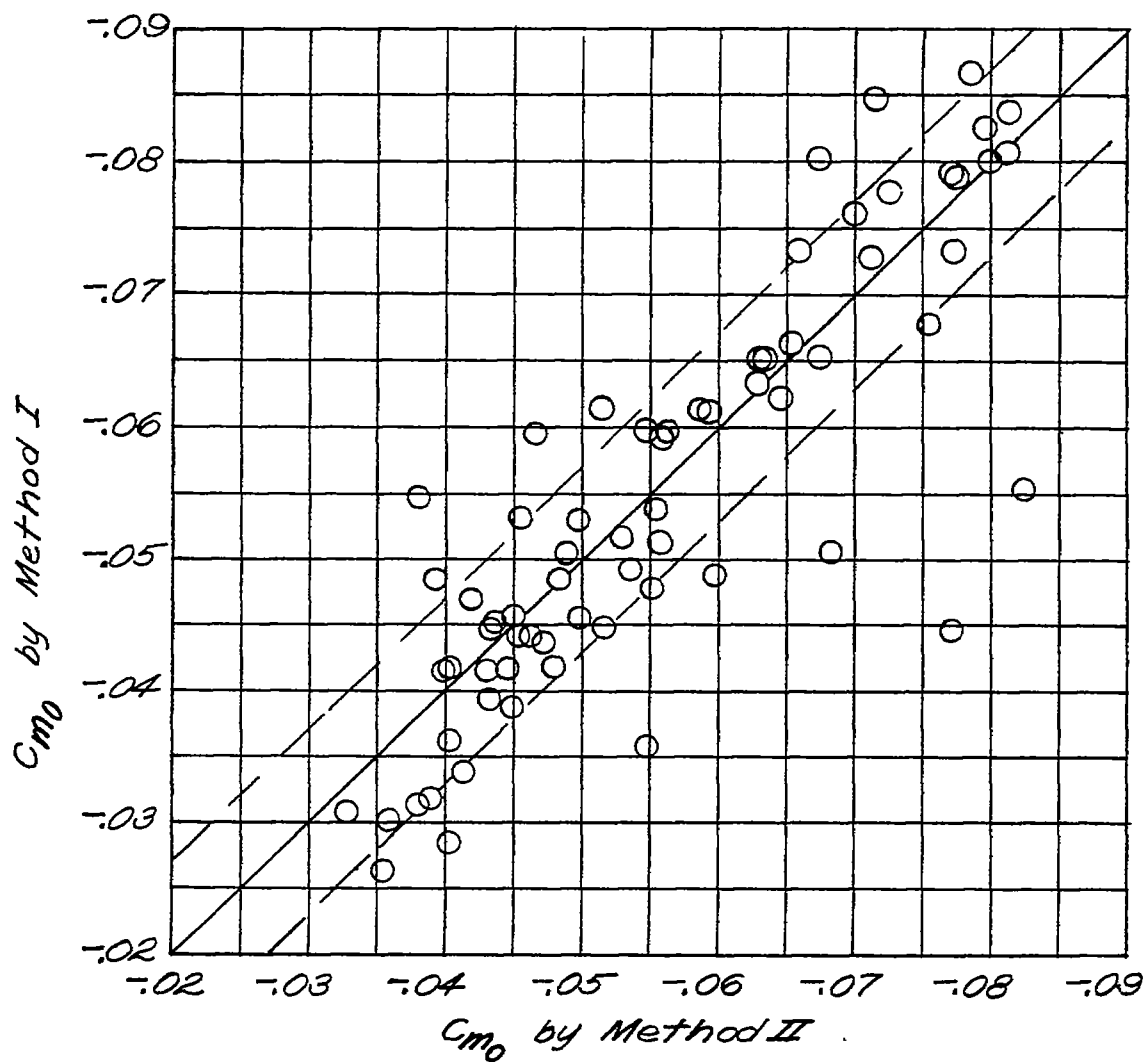
Figure 12.- Comparison of zero-lift wing-fuselage pitching-moment
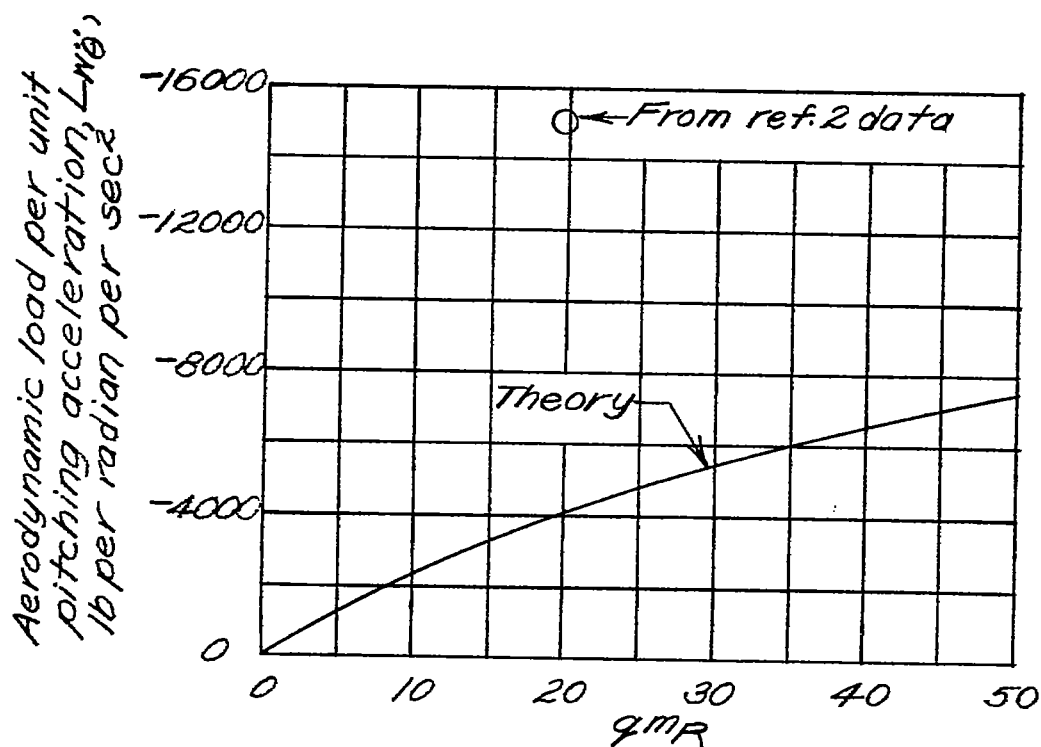coefficients by two methods.
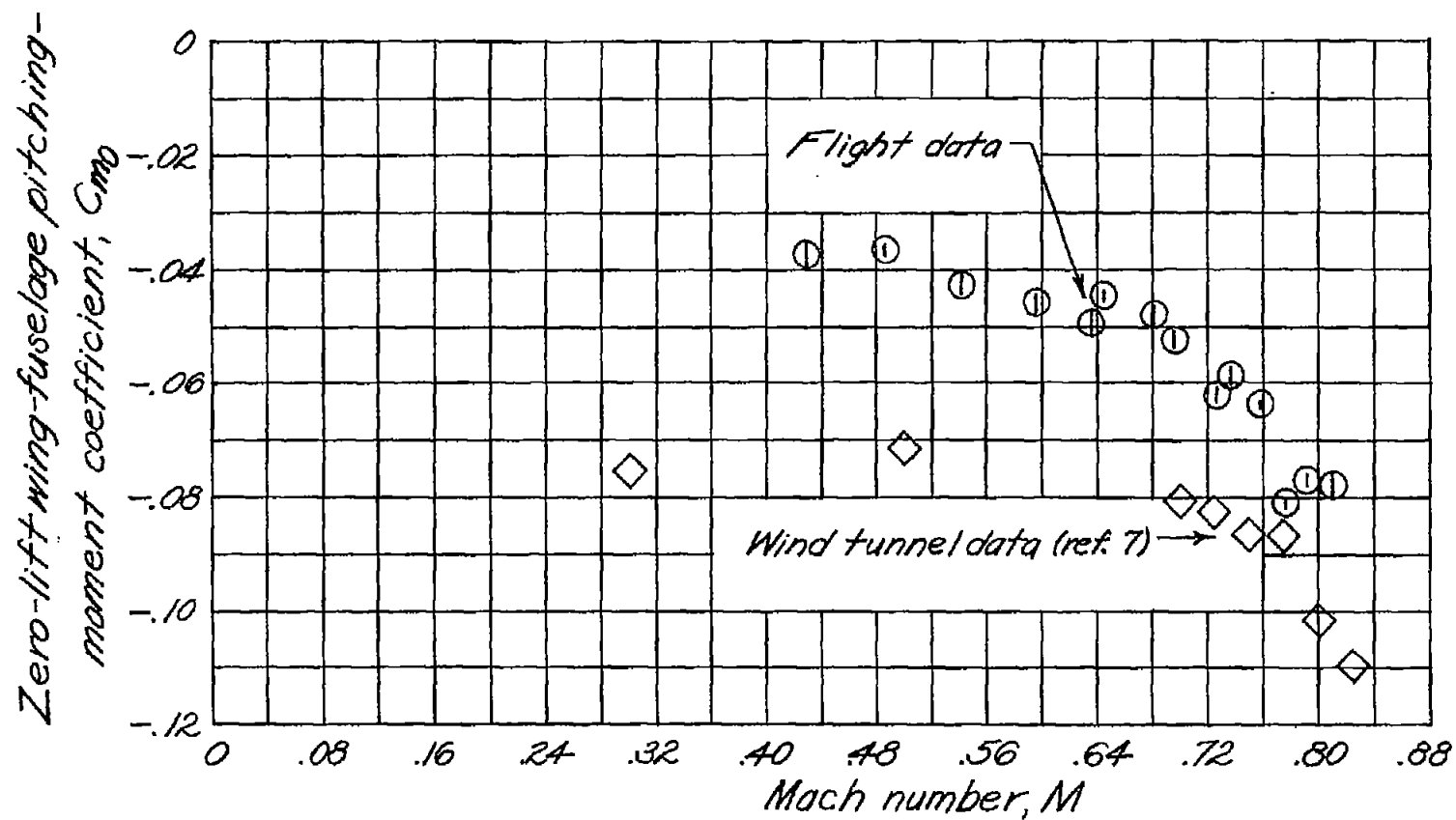
Figure 13.- Comparison of flight and wind-tunnel zero-lift wing-fuselage pitching-moment coefficients. Vertical lines in circle symbols are values of $\overline{\epsilon c_{m_0}}$ from equation (17).
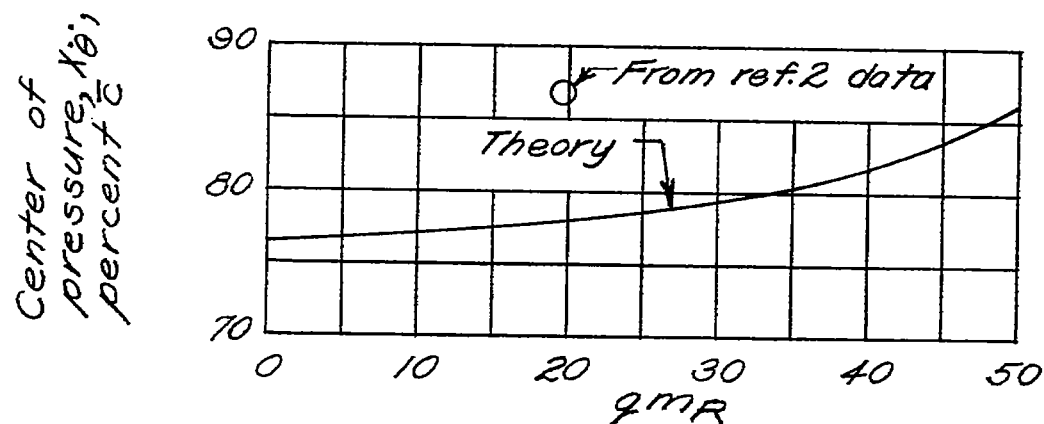
(a) Center of pressure of wing aerodynamic
load due to pitching acceleration.



(b) Aerodynamic load due to pitching
acceleration for both wings.

Figure 14.- Pitching-acceleration wing aerodynamic-load parameters as
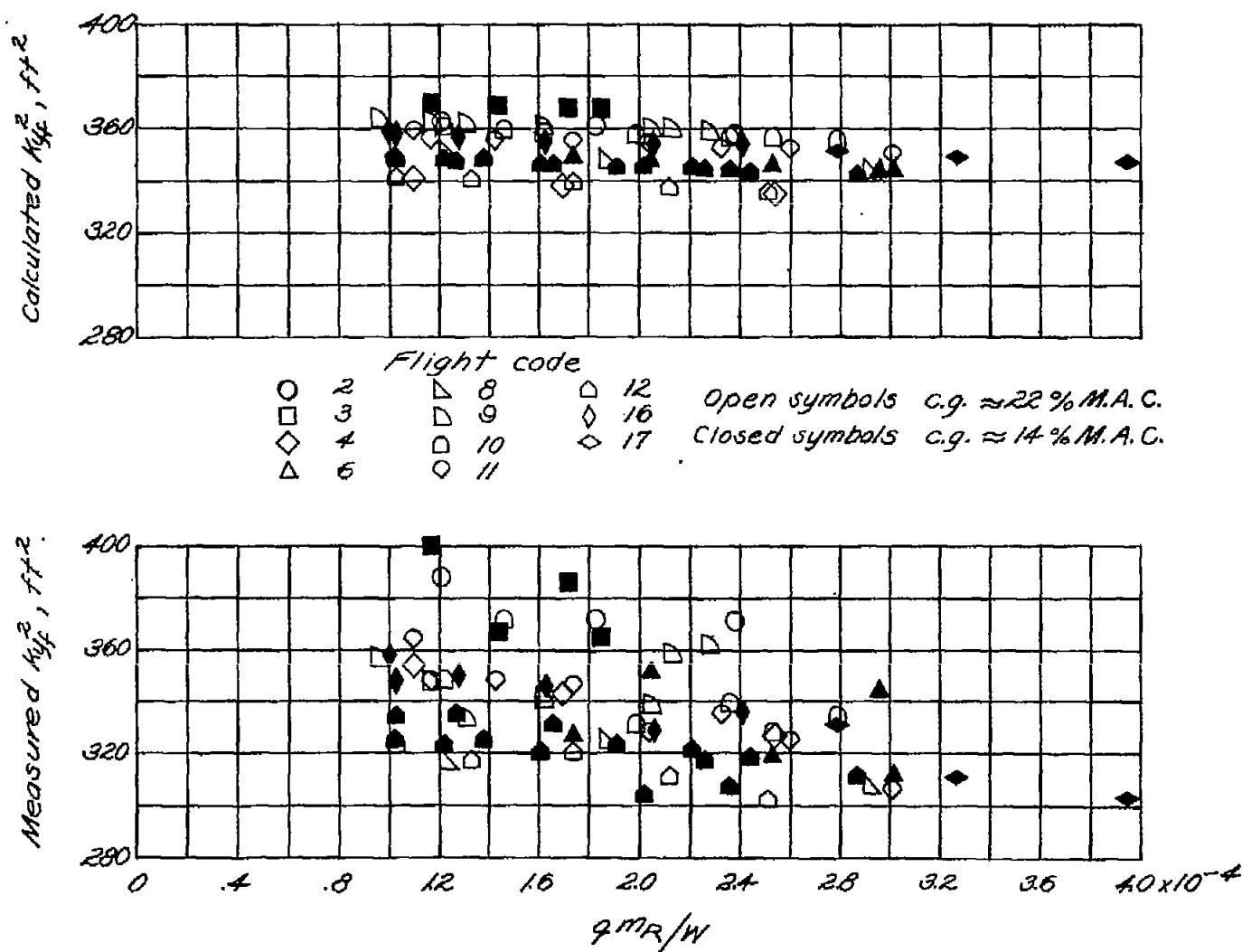functions of flexibility parameter $qm_R$.

Figure 15.- Measured and calculated radii of gyration in pitch squared as function of flexibility parameter $qm_R/W$.